

ISSN 2331-1924

# **International Journal of Computational Intelligence Systems and Applications**

Editor-in-Chief

Prof. Iven Mareels

Volume 3, Number 1 (2015)



**Cayley Nielson Press**

7870 SW NIMBUS AVE, STE775025, BEAVERTON, OREGON, 97008. USA

Ph: 001-503-213-3288, Email: [cayleynielson@hotmail.com](mailto:cayleynielson@hotmail.com)

URL: <http://www.cayley-nielson.com/>

## Journal Information

**Title** : International Journal of Computational Intelligence Systems and Applications

**ISSN** : 2331-1924

**Frequency** : Quarterly

**Website** : <http://www.cayley-nielson.com/ijcisa>

**Publisher** : CAYLEY NIELSON PRESS

**Personal Subscription** : \$50 (Single Journal Copy) \$168 (1-Vol.) \$300 (2-Vol.)

**Institutional Subscription** : \$50(Single Journal Copy) \$192 (1-Vol.) \$360(1-Vol.)

### How to submit manuscript

Submit new manuscript to online submission system on the official website of IJCISA at the [http://www.cayley-nielson.com/ijcisa/paper\\_submission.php](http://www.cayley-nielson.com/ijcisa/paper_submission.php).

### Editor-in-Chief

Prof. Iven Mareels, Melbourne School of Engineering, the University of Melbourne, Australia

Email: mareels.i708@gmail.com

### Co-Chief Editor

Dr. B.M. Cho, Pohang University of Science and Technology, Korea

Email: ko.b.m.cho@gmail.com

### Editors

Prof. P. Wang, Department of Electrical & Computer Engineering, Duke University, USA

Dr. W. Hines, Nuclear Engineering Department, The University of Tennessee, USA

S-M Chen, National Taiwan University of Science and Technology, Taiwan

Prof. M.M. Gupta, Intelligent Systems Research Laboratory, Saskatoon, Canada

Prof. C. Kahraman, Department of Industrial Engineering, Istanbul Technical University, Istanbul, Turkey

Dr. X.Z. Gao, Department of Electrical Engineering, Helsinki University of Technology, Finland

Prof. V. Novak, Institute for Research and Applications of Fuzzy Modeling, University of Ostrava, Czech Republic

Dr. M. Verleysen, Engineering Faculty, University of Louvain, Belgium

### Aim & Scope

The International Journal of Computational Intelligence Systems and Applications, IJCISA, is a refereed journal dedicated to the theory and applications of computational intelligence Systems (artificial neural networks, fuzzy systems, evolutionary computation, expert systems and hybrid systems and so forth). The main goal of this journal is to establish an effective communication channel between researchers involved in the computational intelligence area and developers who use traditional techniques to solve real-world problems, in order to create a worthwhile synergy.

Topics to be considered include, but are not limited to:

- Theory, systems and applications of computational intelligence
- Biologically-inspired computational intelligence
- Computational intelligence in image/signal processing, knowledge discovery
- Evolutionary computation
- Distributed intelligent systems
- Neural systems and human-like agents
- Statistical learning theory
- Related subjects

# INTERNATIONAL JOURNAL OF COMPUTATIONAL INTELLIGENCE SYSTEMS AND APPLICATIONS

ISSN: 2331-1924

Volume 3, Number 1, March 2015

## Contents

The Design and Research of Virtualization Platform <i>Sheng Bai, Yang Liu</i>	1-5
Skeleton Extraction for Real Trees <i>Zhang Dong, Yun Ting, Lianfeng Xue, Honghua Ruan</i>	6-14
Marine Furniture Modeling Based on Kansei Engineering <i>Pei Zhang, Jialu Zhu, Kun Tan, Tong Xu</i>	15-21
Design and Manufacture Cutting Robot Based on AVR Single Chip Microcomputer <i>Qing Zhang, Guikao Yang, Wei Yan</i>	22-25
An Analysis of Influence Factor on Ideal Model Well Testing Curve <i>Yang Chen</i>	26-33
Research on Moving Object Extraction Algorithms Based on Video Sequence <i>Li Cong, Han Fei</i>	34-38
The Construction of Digital Campus Based on City Engine <i>Chao Hui, Ge Xuwen, Jin Feng, Lin Bo, Shi Yali</i>	39-45
Research of Main Arch on Stone Arch Bridge Reinforcement Engineering's Construction Monitoring <i>Hui Yu, Liang Tang, Zhixiang Zhou</i>	46-54
The Summary of Clustering Methods on the Privacy Preserving <i>Shuang Gu, Chi Ma, Bao Li, Meihui Wang</i>	55-61
Experimental Data Publishing Based on Browser/Server for Neutral Beam Injection in EAST <i>Sheng Bai, Yang Liu</i>	62-65



# The Design and Research of Virtualization Platform

Sheng Bai<sup>1</sup>, Yang Liu<sup>2</sup>

<sup>1,2</sup>School of Northeast Petroleum University, Heilongjiang 163318, China

E-mail: <sup>1</sup>*iambaisheng@hotmail.com*

## Abstract

Due to the problem of network structure, security, redundant path in traditional network, this can be solved by Virtual Local Area Network (VLAN) technology. As the network laboratory in colleges and universities is not perfect because of high cost, a virtual simulation tools named Packet Tracer has been introduced to computer network experimental curriculum, this paper put forwards the detail design scheme by the example of VLAN with three switches, and provides the experiment and theoretical analysis and simulation verification. The practice has proved this method not only deepens students' comprehension of network, but also cultivates the students' actual comprehensive ability.

**Keywords:** Network Connectivity, Virtual Local Area Network, Simulation Result, Visual Simulation Emulator.

## 1. Introduction

Computer network is becoming more and more significant in our daily life; it is one of the compulsory course for the computer professional students. Computer network is a closely integrated theory and practice course[1], which emphasis on student's practice operate ability, but it needs lots of money to build network laboratory due to the high cost of network devices[2], so that the perfect network laboratory could not be fully realized in many universities, especially in the process of large complex network, the operate require high performance network entity equipment such as routers and switches, however, the number of students are too much, which can't meet the needs of each student. In order to solve this problem, a virtual simulation tools named Cisco Packet Tracer is introduced into computer network training course[3], which can provide network simulation, visualization and collaboration capabilities. It not only facilitates teaching and learning, but also deepens the understanding of knowledge[4]. The traditional network has the problems [5] of network structure, security, redundant path, which can be solved by Virtual Local Area Network technology. This paper presents the design and implementation example of VLAN in simulation software. This approach is efficient to bring network knowledge to students, this way can help students to open their minds and think graphically.

## 2. Virtual Local Area Network

Virtual Local Area Network is a technology of Virtual teams, which can divide the devices of local area network into small segments, it has the advantages of division flexible, without being limited by the physical location, and VLAN has all the features of a physical network segment. The most representative standard of VLAN frame identification method is IEEE802.1q, the data frame format is shown in table 1.

Lead fram	Separate sign	Target MAC address	Source MAC address	VPID	VCI	Type	Data section	Fram monitoring sequence
7B	1B	6B	6B	2B	2B	2B	46-1500B	4B

**Table 1** Data frame format of IEEE802.1 q

### 3. Experiment Topology Structure

It is necessary to design effective laboratory exercises to cultivate students' innovation. The topology structure diagram is shown in Fig.1, students are asked to build topological structure in Graphical User Interface of Cisco Packet Tracer. It includes three switches, which are named respectively with Switch0, Switch1, Switch2, there are four computers in Fig.1, which are named separately with PC1, PC2, PC3, PC4 from left to right. Meanwhile, PC1 access the fa0/1 port of Switch1, PC2 access the fa0/2 port of Switch1, PC3 access the fa0/1 port of Switch2, PC4 access the fa0/2 port of Switch2. Also, the same devices of switches are connected by cross line, the gigabitEthernet/1 port of Switch1 access the gigabitEthernet/1 port of Switch0, the gigabitEthernet/1 port of Switch2 access the gigabitEthernet/2 port of Switch0, and the port between switches is configured into trunk. At the same time, the IP address configuration and VLAN attributes of computers are shown in tablet.

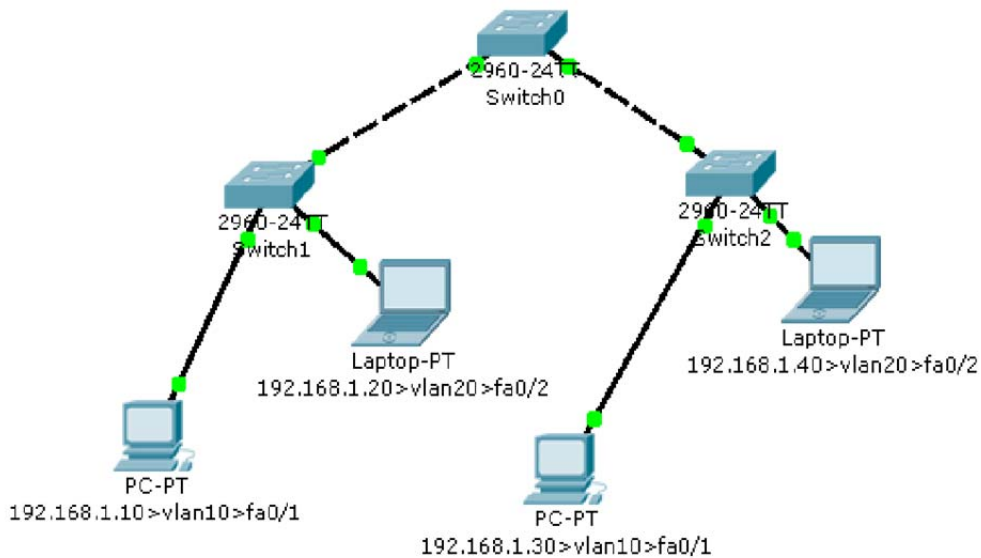


**Fig. 1** The Topology Structure of Network Experiment

Computer	IP address	Subnet mask	VLAN
PC1	192.168.1.10	255.255.255.0	Vlan10
PC2	192.168.1.20	255.255.255.0	Vlan20
PC3	192.168.1.30	255.255.255.0	Vlan10
PC4	192.168.1.40	255.255.255.0	Vlan20

**Table 2** IP address configuration and VLAN attributes

#### 4. VLAN Division

According to Fig. 1, there are two Virtual Local Area Network, V1an10 and V1an20, the division of VLAN is filled into the following steps.

Step one: configure Switch1, divide fa0/1 port into V1an10, divide fa0/2 port into V1an20.

```
Switch1# configure terminal
Switch1(config)#vlan 10
Switch1 (config-vlan)#exit
Switch1(config)#vlan 20
Switch1(config-vlan)#exit
Switch1(config)# interface fastEthernet 0/1
Switch1(config-if)#switchport access vlan 10
Switch1(config-if)#exit
Switch1(config)# interface fastEthernet 0/2
Switch1(config-if)#switchport access vlan 20
Switch1(config-i f)#exit
Switch1(config)#interface gigabitEthernet 1/1
Switch1(config-i f)#switchport mode trunk
```

Step two: configure Switch2, divide fa0/1 port into V1an10, divide fa0/2 port into valn20

```
Switch2#configure terminal
Switch2(config)#vlan 10
Switch2(config-vlan)#exit
Switch2(config)#vlan 20
Switch2(config-vlan)#exit
Switch2(config)# interface fastEthernet 0/1
Switch2(config-if)#switchport access vlan 10
Switch2(config-if)#exit
Switch2(config)# interface fastEthernet 0/2
Switch2(config-if)#switchport access vlan 20
Switch2(config-if)#exit
Switch2(config)#interface gigabitEthernet 1/1
Switch2(config-if)#switchport mode trunk
```

Step three: configure Switch0

```
Switch0#configure terminal
Switch0(config)# interface gigabitEthernet 1/1
Switch0(config-if)#switchport mode trunk
Switch0(config-if)#exit
Switch0(config)# interface gigabitEthernet 1/2
Switch0(config-if)#switchport mode trunk
Switch0(config-if)#exit
Switch0(config)#vlan 10
Switch0(config)#vlan 20
```

### 5. Simulation Result

Due to the principle of hosts can visit each other in the same Virtual Local Area Network; hosts cannot visit each other in the different Virtual Local Area Network. According to Fig. 1, PC1 and PC3 are belonged to same VLAN, PC1 and PC2 are belonged to different VLAN, the result of connectivity between computers is shown in table3, take an example of PC1, the connectivity simulation result of PC1 is shown in Fig.2.

```

PC>ipconfig

IP Address. . . . . : 192.168.1.10
Subnet Mask . . . . . : 255.255.255.0
Default Gateway. . . . . : 0.0.0.0

PC>ping 192.168.1.30

Pinging 192.168.1.30 with 32 bytes of data:

Reply from 192.168.1.30: bytes=32 time=250ms TTL=128
Reply from 192.168.1.30: bytes=32 time=125ms TTL=128
Reply from 192.168.1.30: bytes=32 time=125ms TTL=128
Reply from 192.168.1.30: bytes=32 time=125ms TTL=128

Ping statistics for 192.168.1.30:
    Packets: Sent = 4, Received = 4, Lost = 0 (0% loss),
    Approximate round trip times in milli-seconds:
        Minimum = 125ms, Maximum = 250ms, Average = 156ms

PC>
    
```

**Fig.2** The connectivity result between PC1 and PC3

Computers	Connectivity
PC1 and PC2	no
PC1 and PC3	yes
PC1 and PC4	no
PC2 and PC3	no
PC2 and PC4	yes

**Table 3** The connectivity results

### 6. Conclusion

In computer network course, due to the high cost of network laboratory, many colleges and universities mainly adopt virtual simulation simulator, which can simulate the real network device environment, so that students can experience the configuration process of equipment. This paper gives the design and implementation process example of VLAN, practice shows that this way can deepen the understanding of VLAN. This method is available for teaching and learning.

### References

[1] Zhiqiu Qu, Yue Zhou, Research on application of virtualization in network technology course ,2012 7th International Conference on Computer Science & Education, ICCSE (2012)3 57-359



- [2] Hsin-Ke Lu, Peng-Chun Lin, Effects of interactivity on students' intention to use imulation-based learning tool in computer networking education,2012 14th International Conference on advanced Communication Technology, ICACT, (2012)573-576.
- [3] Frezzo D.C., Behrens J.T., Mislevy R.J., WesP., DiCerbo K.E., Psychometric and Evidentiary Approaches to Simulation Assessment in Packet Tracer Software Networking and Services,2009 Fifth International Conference on Networking and Services, ICNS,(2000)555-560.
- [4] Fuguo Li, Study on security and prevention strategies of computer network, 2012 International Conference on Computer Science and Information Processing, CSIP, (2012)645-647.
- [5] Ruiying Li, Ning Huang, Shuo Li, Rui Kang, Shuo Chang, Reliability testing technology for computer network applications, Proceedings of 2009 8th International Conference on Reliability, Maintainability and Safety, ICRMS, (2009)1169-1172.



## Skeleton Extraction for Real Trees

Zhang Dong<sup>1</sup>, Yun Ting<sup>2</sup>, Lianfeng Xue<sup>3</sup>, Honghua Ruan<sup>4</sup>

<sup>1</sup>Rubber Research Institute, Chinese Academy of Tropical Agricultural Sciences, Danzhou 571737, China.

<sup>1</sup>Department of Information Science and Technology, Nanjing Forestry University, Nanjing 210037, China

<sup>1</sup>Joint Center Sustainable Forestry Studies in Southern China, Nanjing Forestry University, Nanjing Jiangsu, China

<sup>2</sup>Rubber Research Institute, Chinese Academy of Tropical Agricultural Sciences, Danzhou 571737, China.

<sup>2</sup>Department of Information Science and Technology, Nanjing Forestry University, Nanjing 210037, China

<sup>3</sup>Department of Information Science and Technology, Nanjing Forestry University, Nanjing 210037, China

<sup>4</sup>Joint Center Sustainable Forestry Studies in Southern China, Nanjing Forestry University, Nanjing Jiangsu, China

<sup>2</sup>Corresponding author

**E-mail:** <sup>2</sup>285201972@qq.com

### Abstract

The curve skeleton extraction for a given laser-scanned real-tree model plays an important role in many agricultural and forestal applications, such as modeling, parameter measurement and growth simulation. To extract the curve skeletons of real trees, which can capture the essential topology structures, a simple and robust algorithm based on point cloud contraction using constrained Laplacian smoothing is proposed in this paper. The adaptive sampling and post-processing steps designed for complex trees can effectively reduce the computation time and reconstruct the correct curve skeleton from a contracted point cloud. The algorithm of this paper has proved to have better reconstruction effect through Michelia and flowering cherry. The experimental results show that the curve skeletons extracted by this algorithm are faithful and smooth, and they can be well utilized in many fields.

**Keywords:** Tree Skeleton; Forestry; Point Cloud; Laplace Transform; Arithmetic.

### 1. Introduction

With the great development of computer graphics techniques, Three-Dimensional(3D) related applications are becoming much more popular in computer generated worlds. A lot of large and complex objects can be scanned conveniently due to the increasing availability and power of range scanners[1-3]. Trees are very common but vital objects in the natural environment. Research on tree models is beneficial to other fields, such as forestry and ecosystems [4,5]. Unlike other vegetation models, a real tree model, which often consists of a trunk and many densely intricate branches, is very difficult to handle. Besides the complexity of trees, another troublesome fact is that different kinds of trees have different characteristics. Therefore, computing the curve skeletons of various tree models is a challenge in digital agricultural research[6]. Trees' skeleton is the subset of one-dimensional skeleton's medial axis without endpoints[7]. Target in this study is point cloud, compared with the grid model, the reconstruction of trees'

skeleton is far more difficult due to the diversity and uncertainty, because of point cloud has less information and more complicated topology. Although many methods for skeleton extraction have been studied over the past decades [8-11], there are few papers on real trees.

Amenta and others have proposed a geometrical method based on Voronoi in reference[12,13]. This method can process point data directly, but it is sensitive to noise data and it may easily deform the skeleton. Besides, Verrost and other researchers have put forward level-set based method in reference[14], which has no practicability to real trees, because it is sensitive to the noise and easy to miss details. Sharf and others have proposed a method based on variable model evolution in reference [15], which was used to point cloud and polygonal mesh. There are also other methods to get the skeleton of models. The method named thinning through iteration to get the boundary of the voxel to extract the model of the skeleton[16,17], because of the great amount of data, so the whole process was so time-consuming. The method which was based on distance-field defined a distance function in the model space and sited a threshold. Then choosing some points conform to the threshold of distance, the final connection into curve[18-20]. To sum up, there are three difficulties in extracting curve skeletons of trees. One is that obtaining a point cloud by laser scanning is not always easy to implement. Because of the complex branches and leaves, scanned data are always noisy or incomplete, which is intractable for algorithms. Another is that the algorithm should be robust enough to cope with the diversity of point cloud trees and the differences in applications, such as modeling and animation. Last and the most important one is that the above methods are all for the virtual trees or some simple topological structure models. However, there are few methods extracting the curve skeletons on real trees.

In this paper, we present a novel algorithm for extracting the curve skeletons of real trees. Without reconstructing the surface, the proposed algorithm is implemented directly on the point cloud. First, the model is iteratively contracted to a skeletal shape on the basis of the famous constrained Laplacian smoothing method [21]. In this step, the endpoints of branches that act as anchor points are retained at their original positions. Then with an adaptive sampling procedure, the tree model is reduced to a simpler one, where the branches have fewer sample points than the crotches. In order to obtain a 1-D skeleton, a graph is constructed from the sample points and then refined carefully. With this well designed refinement, the curve skeletons of tree models can be constructed correctly. Finally, a post-processing with smoothing operation is implemented on the current curve skeleton. Fig.1 shows the main process of this extraction algorithm. Some classical tree models, including those of michelia trees, cherry trees and soapberry trees, are tested in this paper. The experimental results show the high quality curve skeletons extracted by this algorithm, even for noisy or incomplete models. The operations designed carefully for trees can deal with point clouds successfully.

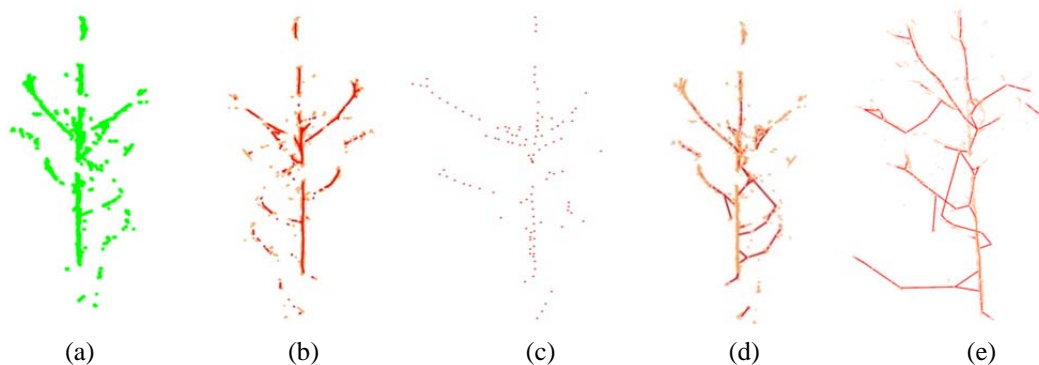


Fig. 1. The main process of extraction.

(a) Point cloud before (orange), (b) after (red) contraction. (c) Adaptive sampling. (d) Constructing and refining graph. (e) Curve skeleton of the corn tree model. (For interpretation of the references to colour in this figure legend, the reader is referred to the web version of this article.)

## 2. Methods

### 2.1 Geometric contraction

The operation of geometric contraction of the point cloud is implemented on the basis of implicit Laplacian smoothing, which removes details and noise from the input data [22,23]. The original points move along their normal directions which are approximated by a constructed 1-ring structure [24]. The algorithm automatically selects some anchor points as feature points, which are fixed to avoid degeneration during the contraction process. These points provide the attraction forces for maintaining the original shape of the input object. After the iterative smoothing, the point cloud becomes a skeletal shape which looks like a curve skeleton. Note that we must firstly construct a 1-ring structure for every point, which is important for computing its normal direction with the Laplacian matrix. To achieve this end, we find the  $k$  nearest neighbors of point  $p_i$  and project them onto its tangent plane. Then a planar Delaunay triangulation of these points can be constructed easily, and the 1-ring neighbors of point  $p_i$  can be naturally defined. As stated in [25], we briefly show the iterative contraction process as follows, where  $t$  is the iteration step:

(1) Solve  $P^{t+1}$  through  $\begin{bmatrix} W_L^t L^t \\ W_H^t \end{bmatrix} P^{t+1} = \begin{bmatrix} 0 \\ W_H^t P^t \end{bmatrix}$ , where  $L$  is a  $n \times n$  Laplacian matrix with

cotangent weights,  $P$  is the contracting point cloud,  $W_L$  and  $W_H$  are the diagonal weight matrices balancing the contraction and attraction forces.

(2) Update  $W_L$  and  $W_H$  by using  $W_L^{t+1} = S_L W_L^t$  and  $W_H^{t+1} = W_H^0 S_i^0 / S_i^t$ , where  $S_i^t$  and  $S_i^0$  are the current and original neighborhood extents of point  $p_i$  respectively.

(3) Construct the new Laplacian matrix  $L^{t+1}$  with the new point cloud  $P^{t+1}$ . We set the neighborhood extent of a point as the average length of its adjacent points. The iteration stops when the solution converges. Most models in our experiments achieve their convergence within a small number of iterations. See Fig. 2 for the result of each iteration step. The point cloud becomes thinner and thinner and finally becomes a skeletal shape.

### 2.2 Adaptive sampling

Since the contracted point cloud  $Q$  has the same number of points as the original one  $p$ , a sampling procedure is necessary for reducing it to a reasonable range. We choose the farthest-point sampling method, which uses a ball of adaptive radius to generate a sampled point set  $G$  with simplified points but approximating well the geometry of  $Q$ . As we know, a tree model always consists of one trunk and many intricate branches, and the branches are connected by the crotches. Hence, in the contracted model  $Q$ , the branches that look like 1D curves need to be sampled by a big radius ball, while the crotches need to be sampled densely to preserve the topology.

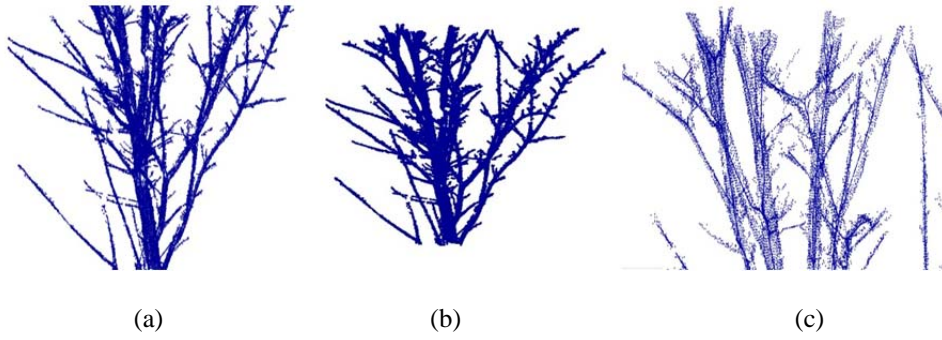


**Fig. 2.** Contraction iteration results. (a) One iteration. (b) Two iterations. (c) Three iterations.

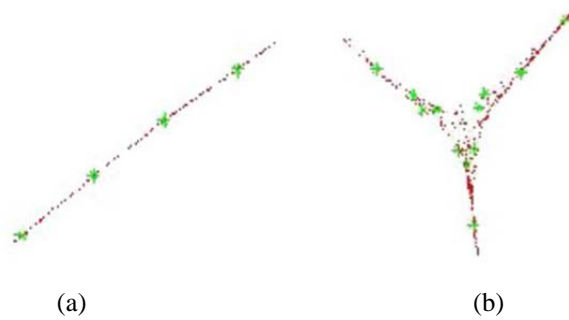


**Fig. 3.** Local adaptive sampling. (a) Sampling at a branch. (b) Sampling at a crotch.

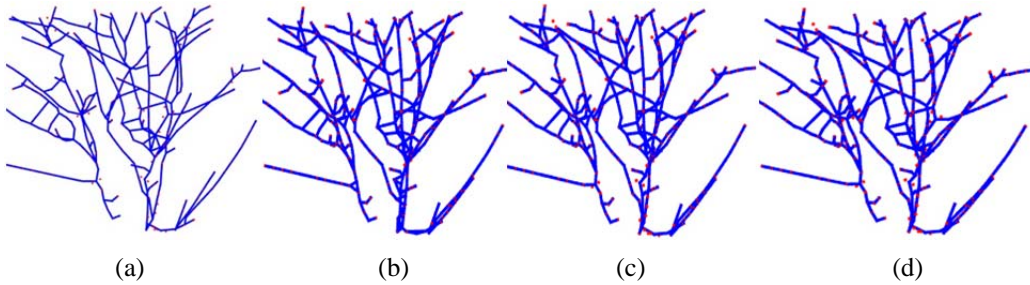


**Fig. 4.** Adaptive sampling with different radii. ((a)–(d)) Sampling results with different radii, from big to small successively.

In order to ascertain whether the current point  $V$  locates on a branch or a crotch, we introduce a value  $L(v)$  for the point set  $V$  included in the sampling ball to describe the current linear trend of  $V$ . Inspired by Pauly et al. [13], we define  $L(v)$  in terms of the eigenvalues of the  $3 \times 3$  covariance matrix  $C$  for  $V$  as follows:

$$L(v) = \frac{\lambda_2}{\lambda_1 + \lambda_2 + \lambda_3} \quad (1)$$

$$C = \begin{bmatrix} v_1 - \bar{v} \\ v_k - \bar{v} \end{bmatrix} \cdot \begin{bmatrix} v_1 - \bar{v} \\ v_k - \bar{v} \end{bmatrix} \quad (2)$$

where we assume  $\lambda_0 \leq \lambda_1 \leq \lambda_2$ . In our test,  $V$  locates on a branch when  $L(v)$  is larger than 0.9; see Fig. 3(a). Otherwise, it locates on a crotch; see Fig. 3(b). To alleviate the influence of the width of  $V$ ,

we carefully set the local sampling radius  $r$  to initially take a large value  $r_{\max}$  and decrease it until  $L(v) > 0.9$ . The decreasing process breaks down if  $r$  is smaller than a given threshold  $r_{\min}$ , which means that the current point  $V$  is a crotch point, and we set the local sampling radius  $r = r_{\min}$ . Using this adaptive sampling method,  $G$  has minor points on branches and major points at crotches, and forms a similar shape to the input object  $Q$ . Fig. 4 gives the results after adaptive sampling with different radii of the sampling ball. The smaller the radius, the greater the number of points sampled, especially at the crotches.

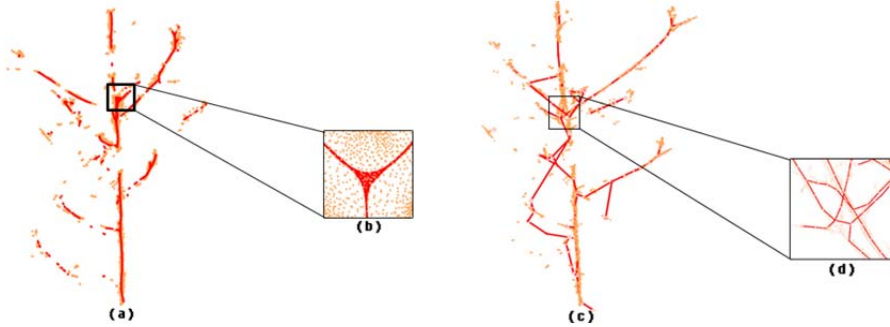


**Fig. 5.** Constructing and refining the graph. (a) Graph construction. (b) Close-up of (a). (c) Graph refinement. (d) Close-up of (c).

### 2.3 Graph construction and refinement

$G$  consists of a small number of points, which can represent the shape of the original object. However, there is no connectivity among these isolated points. So we first construct an incomplete graph on  $G$  and then refine it carefully to generate a 1D curve skeleton. In the rest of this paper, we call the sample points ‘nodes’ to avoid confusion. Given two nodes, each of them represents a subset of  $p$  due to the farthest-point sampling. The 1-rings of those subsets are considered. If they share common points, it means the two nodes are near enough, so an edge is constructed between them. After the implementation for every two nodes in this manner, we obtain a graph that looks like the skeleton but has some redundant edges. Fig. 5(a) shows an example of the constructed graph, and Fig. 5(b) is the close-up of the result. For the purpose of eliminating those useless edges, the graph is refined in the next step. Two kinds of edge operators are defined: merging operators and removing operators. Generally speaking, tree models do not have cycles, so we collapse unnecessary edges until no cycles exist in  $G$  to build a curve skeleton graph. The degree of an edge is defined as the maximum degree of its two endpoints. We iteratively collapse the edge with the highest degree in a cycle. If there are many edges with the highest degree, we collapse the one with minimum Euclidean length. In each step, we merge the two endpoints to their midpoint, or remove the edge, according to the distance between the two represented points of the two endpoints. When their distance is smaller than a given threshold  $T$ , the edge is collapsed by using the merging operator. Otherwise, the removing operator is utilized. The represented point set of the nodes is updated after the merging operation. Fig. 5(c) is an initial curve skeleton obtained after refining the graph, and Fig. 5(d) is the close-up of the result.

### 2.4 Post-processing

The curve skeleton  $G$  obtained by the previous steps is almost a perfect one, except for its smoothness. The last step is a post-processing including the smoothing operation. We use the least square

method [14] to smooth the skeleton  $G$  because of its simplicity. The Laplacian energy of  $G$  is utilized as the smoothing constraint, and the mean position of the represented points is utilized as the approximation term. Besides, the same surgeries as are presented in [15], performed to deal with some imperfections, for example removing redundant short edges, are implemented on the skeleton too. With all of the previous computations, a curve skeleton that has the same shape as the input model is produced successfully. Fig. 1(d) shows a good result for extracting the curve skeleton of the corn tree model.

### 3. Results and discussion

We show examples demonstrating our curve skeleton extraction technique on a range of tree models, which have hundreds of thousands of points. In all experiments, the curve skeletons are extracted automatically within a few seconds.

Besides the corn tree model presented in previous sections, here we take three other kinds of tree models as examples in order to show the robustness of our algorithm. In these examples, some tree models are complete point clouds, while others are not such as the cherry tree model. The results demonstrate that our algorithm can deal with both complete and incomplete point clouds well. For visualization, the original points are shown in orange, while the final skeleton is shown in red.

In all experiments, we set  $k = 0.02 \times n$ , but restrict the values to the range  $[10, 30]$ , where  $n$  is the sample number for the original model. The restriction is set because we only need a 1-ring neighbor of every point in the tree model. If  $k$  is too big, the 1-ring neighbor of one branch point will extend to the other branches.

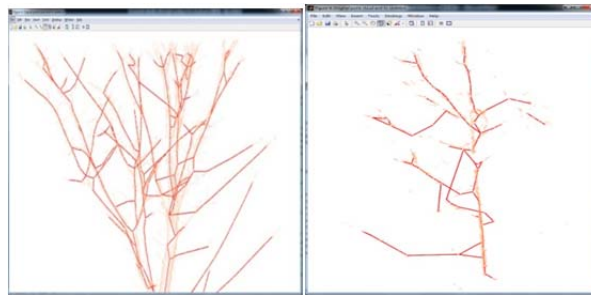


Fig. 6. The skeletons of the cherry tree and Michelia tree.

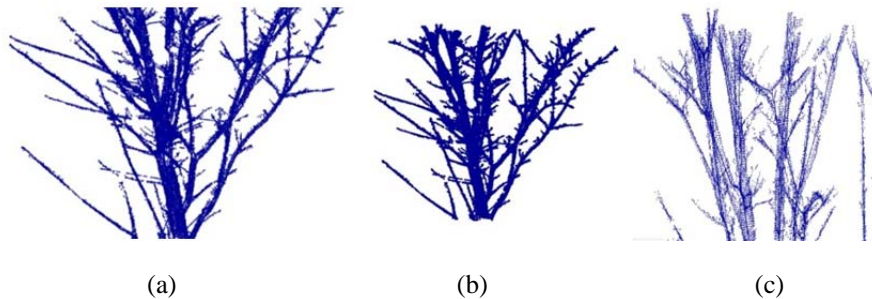


Fig. 7 The influence of  $s_l$ . Let  $w_l^0 = 1.0$ ,  $w_h^0 = 1.0$  and iterate 2 times.  $S_l$  is respectively select value as 0.5, 1, 2 from figure (a) to (c).



**Table 1** The experimental parameters of the Flowering- Cherry

Test number	Update intensity	Contraction intensity	Control intensity
1	0.5	1	3
2	1	1	3
3	2	1	3

**Table 2** Experimental parameters on Michelia

Test number	Updates intensity	Contraction intensity	Control intensity
1	2	0.5	3
2	2	1	3
3	2	2	3

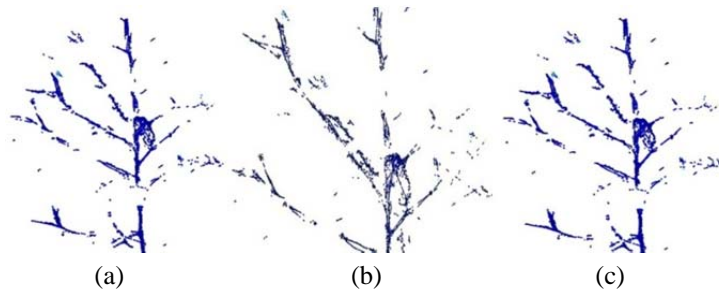


**Fig. 8** The influence of  $w_h^0$ . Let  $w_t^0 = 1.0$ ,  $w_h^0 = 3.0$  and iterate 2 times.  $w_h^0$  is respectively select value as 0.5, 1, 2 from figure (a) to (c).

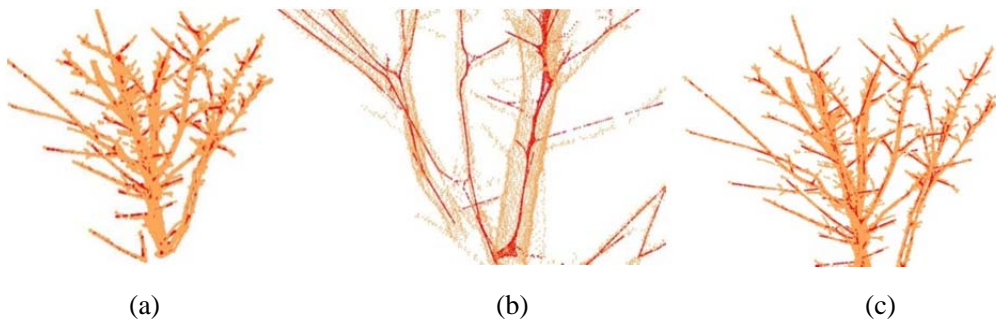


**Fig. 9** The influence of  $w_L^0$ . Let  $w_L^0 = 1.0$ ,  $w_H^0 = 3.0$  and iterate 2 times.  $w_L^0$  is respectively select value as 1, 3, 5 from figure (a) to (c)

In the contraction process, we set  $S_L = 2$ , and  $W_L = W_L = 1$  to obtain a good skeletal shape in a few iterations. In the adaptive sampling and graph refinement process, we set  $r_{max} = 100 \times d$ ,  $r_{min} = 10 \times d$ ,  $T = 25 \times d$ , where  $d$  is the average distance of points in  $P$ . Fig. 6 shows the results for the plum tree, apple tree and cherry tree models. On the basis of the analysis and results demonstrated above, we can conclude that our algorithm is effective and robust for extracting the curve skeletons of tree models.

#### 4. Conclusion

With constrained Laplacian smoothing, adaptive sampling and skeleton reconstruction, a curve skeleton extraction algorithm for tree models is presented. According to the special structure characteristic of tree models, we design a series of well-targeted tricks in order to extract a smooth and faithful skeleton. Any given tree model is contracted to a thinner one which maintains the global shape of the input model by anchoring points chosen automatically. After adaptively sampling some representative nodes in order to reduce the complexity, a graph is constructed and refined successively. Finally, a post-processing step is implemented, which results in a better curve skeleton. Our method is robust to noise and sample distribution, and can deal with the general missing data problem that is commonly encountered in scanning big tree models. Further, special tricks like adaptive sampling and cycle elimination are designed for particular characteristics of tree models. The experimental results demonstrate the effectiveness of our algorithm with different kinds of tree models. The extracted skeleton is very smooth, so it can be conveniently utilized in many other applications. Besides, every point in the curve skeleton represents a small point cloud of original data, which is an important condition in retrieval and animation. The main limitation of this algorithm is the low efficiency when dealing with extremely luxuriant tree models. In future, we would like to overcome this shortcoming by improving the neighborhood construction method.

#### Acknowledgments

Disclaimer: Views expressed in this article are those of the authors and do not have any dispute. This work is supported by national Natural Science Foundation of China (31300472), Natural Science Foundation of Jiangsu Province (BK2012418, BK2012815), Opening Project Fund (RRI-KLOF201501) of Key Laboratory of Rubber Biology and Genetic Resource Utilization, Ministry of Agriculture. Meanwhile, we appreciate for the experimental devices provided by National Basic Research Program of China (973 Program, 2012CB416904) and Priority Academic Program Development of Jiangsu higher education Institutions.

#### References

- [1] Amenta N., Choi S, Kolluri RK (2001). The power crust, unions of balls and the medial axis transform. *Comput Geom* 19: 127-153.
- [2] Verroust A., Lazarus F (2000) Extracting skeletal curves from 3D scattered data. *Vis Comput* 16: 15-25.
- [3] Weber C., Hahmann S, Hagen H (2010) Sharp feature detection in point clouds. In: *Proceedings of the 2010 IEEE International Conference on Shape Modeling and Applications (SMI '10)*. pp. 175-186.
- [4] Smith SM, Brady JM (1997) A new approach to low level image processing. *Int J Comput Vis* 23: 45-78.
- [5] Milnor JW (1963) *Morse theory*. Princeton: Princeton University Press.
- [6] Tenenbaum JB, de Silva V, Langford JC (2000) A global geometric framework for nonlinear dimensionality reduction. *Science* 290: 2319-2323.
- [7] Blum HA (1967) Transformation for extracting new descriptors of shape. In: *Wathen-Dunn W, editor. Models for the perception of speech and visual form*. Cambridge, MA: M.I.T. Press. pp. 362-380.
- [8] Wu FC, Ma WC, Liou P, Liang RH, Ouhyoung M (2003) Skeleton extraction of 3D objects with visible repulsive force. In: *Proceedings of the Eurographics Symposium on Geometry Processing*. pp. 1-7.
- [9] Kimmel R, Sethian JA (1998) Computing geodesic paths on manifolds. *Proc Natl Acad Sci U S A* 95: 8431-8435.

- [10] Mémoli F, Sapiro G (2001) Fast computation of weighted distance functions and geodesics on implicit hyper-surfaces. *J Comput Phys* 173: 730-764.
- [11] Bertrand G, Aktouf Z (1994) A three-dimensional thinning algorithm using subfields. In: Proceedings of the SPIE Conference on Vision Geometry, Vol. 2356. pp. 113-124.
- [12] Baldocchi D. (2013) 4.08 - Ecosystem services of energy exchange and regulation. In: Pielke RA, editor. *Climate Vulnerability*, Vol. 4: *Vulnerability of Ecosystems to Climate*. Oxford: Academic Press. pp. 81-92.
- [13] Bennett, ND, Croke BFW, Guariso G, Guillaume JHA, Hamilton SH, et al. (2013) Characterising performance of environmental models. *Environ Model Softw* 40: 1-20.
- [14] Wei J, Salyani M (2005) Development of a laser scanner for measuring tree canopy characteristics: Phase 2. Foliage density measurement. *Trans ASAE* 48: 1595-1601.
- [15] Llorens J, Gil E, Llop J, Queraltó M (2011) Georeferenced LiDAR 3D vine plantation map generation. *Sensors (Basel)* 11: 6237-6256.
- [16] Bruce JW, Giblin PJ (1992) *Curves and singularities*, 2nd ed. Cambridge: Cambridge University Press.
- [17] Preparata FP, Shamos MI (1990). *Computational Geometry, Texts and Monographs in Computer Science*. New York: Springer-Verlag.
- [18] Kovács I, Julesz B (1994) Perceptual sensitivity maps within globally defined visual shapes. *Nature* 370: 644-646.
- [19] Lee TS, Mumford D, Schiller PH (1995) Neural correlates of boundary and medial axis representation in primate striate cortex. *Invest Ophthalmol Visual Sci* 36: S477.
- [20] Ogniewicz RL (1993) *Discrete Voronoi skeletons*. Zurich: Hartung-Gorre Verlag Konstanz.
- [21] Serra J (1982). *Image analysis and mathematical morphology*. New York: Academic Press.
- [22] Blum H (1973) Biological shape and visual science. *J Theor Biol.* 38: 205-287.



## Marine Furniture Modeling Based on Kansei Engineering

Pei Zhang<sup>1</sup>, Jialu Zhu<sup>2</sup>, Kun Tan<sup>3</sup>, Tong Xu<sup>4</sup>

<sup>1</sup>Title of the institution, city, country College of Mechanical and Electrical Engineering, Harbin Engineering University, Harbin 150001, China

<sup>2</sup>School of Education, Shanghai International Studies University, Shanghai 201620, China

<sup>3,4</sup>Title of the institution, city, country College of Mechanical and Electrical Engineering, Harbin Engineering University, Harbin 150001, China

**E-mail:** <sup>1</sup>1196320696@qq.com, <sup>2</sup>lenkachu125@gmail.com, <sup>3</sup>1148469586@qq.com, <sup>4</sup>605522188@qq.com

### Abstract

Kansei Engineering, mainly by the analysis of human sensibility to make products that meeting people's preferences, by application of Kansei engineering theory to consider the emotional response of crewmen and transform the specific phenomena such as emotional reactions into design elements, to design marine furniture that meet the crew's use and preference. Reaching marine furniture design optimization, improving ship design level internal environment, maximizing the use of internal ship space, so as to create a more comfortable living environment for the crew, bringing more natural psychological feelings and providing a reference for subsequent modeling studies of marine furniture.

**Keywords:** Marine Furniture, Kansei Engineering, Modeling Research.

### 1. Introduction

Kansei engineering is by exploring the relationship of the elements of product design and the consumer emotional to research the emotional impact between different users and different products, in order to select the combination of design parameters to maximize consumer satisfaction. Kansei engineering is that using approach based on science to try to quantify the human sensibility (including the "feelings quantity" "feel the amount of" physical and psychological), and find out the amount and variety of the physical sensibility engineering used in the relations between developed and then applied to engineering or design. The principle is shown in Figure 1.1.

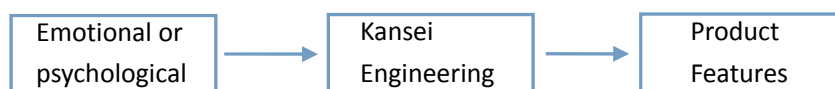


**Figure 1.1** Kansei engineering principle

The earliest men who apply the perceptual analysis into Engineering research area are the researchers of Japan Hiroshima University Faculty of Engineering. In 1970s, at the beginning of fully considering the emotion and desire of the livers, people began to study how to embody the sensibility of the occupants in residential design in engineering technology; this new technology was originally known as "emotional engineering." This term was first proposed by Mazda Motor Group, the former president Kenichi Yamamoto in 1986, published in the University of Michigan, entitled "car culture" theory first proposed speech. From the beginning of 1989, Hiroshima University associate professor of engineering, foreign

minister Sansheng Ting, after years of research, has published a series of papers and works about Kansei Engineering, became famous Japanese Kansei Engineering Research experts.

Kansei Engineering famous Japanese scholar Long-cho Sansei classifies Kansei Engineering credits for perceptual information classification, Kansei Engineering system, hybrid Kansei engineering systems, Kansei Engineering model, virtual Kansei Engineering .Because of Kansei engineering is still in its early stages of development, different Kansei engineering experts' research different directions, and the research methods are quite different. But the problems of implementation of Kansei engineering and design to be solved and the basic method on Kansei Engineering design are the same. The key problems that need to be addressed of Kansei Engineering are:

(1) How to capture the customer perception of the product based on the assessment of ergonomics and psychology;

(2) How to define the design characteristics of the product by the customer's emotional;

(3) How to establish the Kansei Engineering Ergonomics as a technology;

(4) How to adjust the design to meet the changes in society and people's preferences tendencies.

In response to these questions the practice of Japanese researchers are:

(1) the use of Osgood and his colleagues developed by the SD method (semantic differential method) sensibility to capture customers as an important technical means to collect from the market or from the corporate sensibility, magazines, or depicting customer perceptions of vocabulary, usually first collect 600-800 vocabularies which describe emotion, and then choose from nearly 100 of the most relevant vocabularies for analysis;

(2) the investigation or experiment designed to test the sensibility words and design elements of relevance;

(3) use of advanced computer technology to create a systematic framework for sensual works, through the use of artificial intelligence, neural networks and fuzzy logic geometric methods, and the establishment of relevant databases and computer reasoning system;

(4) Every three to four years, by adjusting the perceptual engineering database, expand the new data into the database sensibility, thus to study changes in customer product preferences trend.

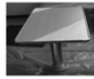









## **2. Marine furniture Research Track sum method**

### **2.1 Furniture localization**

As an important part of marine furniture, ship interior decoration is strict than ordinary land furniture both in the design, material or construction and other aspects. Marine furniture is essential appliance for crew in daily life, the reasonable style not only to adapt to the requirements of crew on life, but also to meet the aesthetic requirements of them so as to improve crew mood. Modeling beautiful and practical furniture will make the crew feel comfortable and relieve their fatigue. Due to the large and complex cabin of ship, positioning in cabin should as far as possible to the comprehensive diversity cabin appropriately process, completes the inductive classification and selection of cabin overall. Product design based on Kansei engineering is to start from the investigation on the needs of target users, design product positioning different, corresponding to the user of the product perceptual cognition, their needs and purchasing power and other aspects may be different. I will take the ship cabin restaurant table in modeling design to studied, the restaurant is a multi-functional interpersonal communication leisure space in order to meet the needs of eating, entertainment, culture, leisure and meetings .Therefore, modeling of dining table is very important.

## 2.2 Choose furniture typical sample cloth

Through the dining room table in furniture stores, research and the brochure of furniture product magazines, ship, network and other ways to collect the sample for collection, select a representative sample of 20 (see table 1), in order to avoid influence of this furniture in the study of perceptual image color factors, and to eliminate the color of the representative sample.

				
1	2	3	4	5
				
6	7	8	9	10

**Table 1** Representative samples





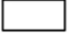





## 2.3 Perceptual semantic space set up

(1) Determine the emotional vocabulary and design elements

Through relevant ads, manuals, documents, reports, etc, to collect the perceptual words, and use the Semantic Differential method (Semantic Differential, SD) to set evaluation. Semantic differential method is invented by the American psychologist and his colleagues. This method is used in the form of paper and pencil, and was asked to be used on several levels of semantic scale at seven o'clock on a certain object to evaluate a concept (such as cars, neighbors) or something, in order to understand the things or concepts in the meaning of each college or dimensions and strength. Level sequences of two endpoints are often the meaning of two different adjectives, such as honesty and dishonesty, strong and weak, important and not important. Under normal circumstances, the more perceptual words collected are not conducive to future study, so they have to be highly generalized, use less and typical vocabulary of the sensibility as far as possible to represent all the perceptual vocabulary. This needs to make the evaluation questionnaire based on the semantic distinction, to evaluate the perceptual words, then using the factor analysis method (factor analysis), Cluster analysis (Cluster analysis)) to research and analyze the results of the survey, perceptual evaluation of vocabulary will eventually be identified as: neat-mixed, simple-tedious, classical-modern, light-heavy, fashion-primitive, clean-dirty, technical-manual, delicate-rough 8 pairs of words (see chart 2). Through the literature and expert elements, including the modeling of the dining room table as: desk, table legs and desktop, the categorize of each element (see table 3).

Neat-Mixed	Simple-Tedious
Classical-Modern	Light-Heavy
Fashion-Primitive	Clean-Dirty
Technical-Manual	Delicate-Rough


**Table 2** Select the adjectives

Design Factor	Classification Simplified Schematic Design Factors			
Table Seat (X1)	 C11 Square	 C12 Circle	 C13 Trapezoid	Others C14
Table Leg (X2)	 C21 Square	 C22 Rectangle	 C23 Circle	 C24 Four Prismatic C25
Table Top (X3)	 C31 Square	 C32 Rectangle	 C33 Circle	

**Table 3** classification of design elements

(2) The questionnaire design

Using semantic differential method to establish magnitude 7 semantic differential scales of the 10 samples selected of dining-room table in black and white and 8 pairs of emotional adjectives eventually set up, to made perceptual evaluation of semantics. (See table 4)



	Neat	3	2	1	0	-1	-2	-3	Mixed
	Simple	3	2	1	0	-1	-2	-3	Tedious
	Classical	3	2	1	0	-1	-2	-3	Modern
	Light	3	2	1	0	-1	-2	-3	Heavy
	Fashion	3	2	1	0	-1	-2	-3	Primitive
	Clean	3	2	1	0	-1	-2	-3	Dirty
	Technical	3	2	1	0	-1	-2	-3	Manual
	Delicate	3	2	1	0	-1	-2	-3	Rough

**Table 4** the questionnaire sample

(3) The questionnaire and data collection

Because of the short time and limited conditions, so we only selected 50 volunteers to scripts to test, in which 30 persons are students of the school of industrial design professional, 2 people are full-time teachers, 13 people are ship furniture designers, 5 people are the person who Aboard the ship many times in coastal areas more staff, let them to evaluate each emotional vocabulary of each sample. Through the EXCEL software processing, get the average of the Emotional semantic evaluation of the subjects to 10 samples of dining-room table, and to make perceptual evaluation matrix combined with the design elements of shape features. (See table 5)



	Design Factor			Perceptual Semantic Evaluation Value							
	X1	X2	X3	Neat-Mixed	Simple-Tedious	Classical-Modern	Light-Heavy	Fashion-Primitive	Clean-Dirty	Technical-Manual	Delicate-Rough
	C12	C23	C32	1.2	0.3	0.2	-0.4	0.2	1	-1.5	-0.2
⋮	⋮	⋮	⋮	⋮	⋮	⋮	⋮	⋮	⋮	⋮	⋮
	C12	C23	C31	1.5	1.3	1.2	1	0.5	1.2	-2	-0.5

**Table 5** perceptual evaluation matrix

(4)The establishment of relations of the Kansei meaning and modeling elements

In the process of converting Kansei Evaluation Scale for the engineering scale can use multiple linear regression analysis, the quantitative theory type I algorithm, neural network, genetic algorithm, rough set analysis method etc. The quantitative theory type I is the most commonly used method. Quantitative theory I class is to study the relation between a group of qualitative variables X (independent variables) and a set of quantitative variables y (the dependent variable) by using multiple linear regression, to establish the mathematical model between them, so as to achieve the observation to variable y. The method is used for Kansei engineering research, often regard the evaluation of Kansei vocabulary as a reference variable value and the form features of product as the dependent variable, and establish the prediction model as the following:

$$Y=G_{ij}C_{ij}+M \tag{1}$$

Type 1, y is the average of perceptual semantic evaluation; G<sub>ij</sub> is the weight coefficient of each independent variable, C<sub>ij</sub> is the response value of other elements (I as design elements, J as category); m is a constant value.The model can be solved using the result of SPSS19.0 statistical software analyzing the multivariate linear regression including partial correlation coefficient, the constant term, categories and other data, the results in Table 6 (simple to tedious, for example), the partial correlation coefficient between the Kansei vocabulary and design project.

Model	Non standardized coefficient		Standardized coefficient	t	Sig.	Correlation			Collinearity statistics	
	B	Std. error				Zero-order	Partial	Parlor	Tolerance	VIF
1 (Constant)	.200	.000		.	.					
C15	5.667	.000	.560	.	.	.663	1.000	.427	.583	1.714
C21	-.778	.000	-.160	.	.	.001	-1.000	-.090	.318	3.147
C22	-1.675	.000	-.221	.	.	-.317	-1.000	-.110	.251	3.991
C23	.667	.000	.425	.	.	.818	1.000	.251	.350	2.857
C31	.667	.000	.313	.	.	.619	1.000	.201	.412	2.429
C33	-.217	.000	-.047	.	.	-.367	-1.000	-.023	.230	4.354

a. Dependent Variable: Simple complex

**Table 6** SPSS software linear regression analysing data

Design Factor	Category	Coefficient of Partial Correlation	The Design Factor Scores	
			Simple	Tedious
Table Seat X1	C11 Square C12 Circle C13 Trapezoid C14 Others	1	Exclude	
			Exclude	
Table Leg X2	C21 Square C22 Rectangle C23 Circle C24 Four Prismatic C25 Others	-0.33	1.636	
			6.212	
				-1.869
				-2.698
			0.558	
Table Top X3	C31 Square C32 Rectangle C33 Circle	1	Exclude	
			Exclude	
			0.667	
			Exclude	
			0.192	
Constant Term	0.364			

**Table 7** the results of analysing the elements of modeling and the adjective "association between simple - complex"

By the design factor score every category effect on Kansei vocabulary and the influences of the direction can be seen, such as the round table leg bias beautiful and rectangular table leg bias tedious. Get the contribution of the size of each design elements to Kansei vocabulary by partial correlation coefficient, its value is high, then contribution is bigger, such as contracted contributions of the desktop to Kansei vocabulary. The function relationship between Kansei beautiful vocabulary and every elements of design is:

$$Y_{\text{simple}} = 1.636 * C13 + 6.212 * C14 - 1.869 * C21 - 2.698 * C22 + 0.558 * C23 + 0.667 * C31 + 0.192 * C33 + 0.364$$

In order to verify the validity of the above function, we can reselect the sample, carries on the questionnaire survey, analysis the data and the prediction function of the investigation of the calculated data by T test, test showed the significant level is greater than 0.05, no significant differences, so the results are reasonable. Similarly, we can get the prediction function of other Kansei vocabulary that present other factor relations on the dining table, the function can judge the kansei image feelings of designer through innovative design to convey, whether consistent with the requirements of the users, and provide basis for trade-offs of design scheme and subsequent in-depth design.

### 3. Conclusion

Kansei Engineering aims to explore the perceptual cognition of people for object, and applies it into the design elements to the new product. Study on marine furniture based on the product design method of Kansei Engineering, reaching the functions of the emotional vocabulary and the element of modelling. These functions contribute to the ship furniture designer design to marine furniture corresponding to sailors, provide a reference for the further research of marine furniture. Using the method in this paper also can analyze the innovative design of the furniture color, material etc, used for auxiliary design and evaluate design effect, so that the careful "coding" perceptual information of designer can get the correct

"decoding" of user for the furniture products, so as to realize the unite of emotional and rational of furniture products.

### **References**

- [1] Yongfeng Li,Liping Zhu.Research on product design method based on Kansei engineering. Packaging engineering,2008.
- [2] Hongbing Zhang.SPSS Collection. Bei Jing: Publishing House of electronics industry, 2007.
- [3] Shijian Luo,Yunhe Pan.The progress of the Kansei image theory,research of technology and application in product design. Chinese Journal of Mechanical Engineering, 2007.
- [4] Qiufang Zhao.Research on Kansei Engineering and its application in the product design. Ji Nan: Shandong University, 2007.
- [5] Long Liu, Jiayi Tang, Jing Gao. Research of automobile interior design Based on Kansei Engineering work process. Modern manufacturing engineering, In 2010 eleventh period.



# Design and Manufacture Cutting Robot Based on AVR Single Chip Microcomputer

Qing Zhang<sup>1</sup>, Guikao Yang<sup>2</sup>, Wei Yan<sup>3</sup>

<sup>1,2,3</sup> Air Force Logistics College, Xuzhou, China

<sup>1</sup>Corresponding author

E-mail: <sup>1</sup>zhangqinglhq@163.com

## Abstract

This paper introduces a kind of dancing robot, through the ATmega16 single-chip microcomputer to control the PWM signal in order to control the steering engine, drive MG945 work, which can make the robot performances paper-cut, make the difficulty and ornamental and action. This system takes the competition task driven, modular design, and the software using C language.

**Keywords:** ATmega16 microcontroller, MG945 actuator.

## 1. The design ideas and standards

The robot based on ATmega16 single chip microcomputer as the main control. The main body is composed of 21 steering part compositions, structure design and improvement of humanoid robot arm in the mechanical structure, can achieve a stable grasp some pre origami, scissors and other complex and graceful movements, to display and promote Chinese folk paper-cut art.

## 2. The system composition and working principle

The hardware of this system are mainly connected with serial debugging circuit, servo control circuit board welding, software mainly completes the robot action program debugging and downloading functions [1]. Through the ATmega16 single-chip microcomputer to control the output PWM signal to control the rudder rotation, realizes the robot to the smooth operation of paper-cut art. The system structure diagram as shown in figure 1.

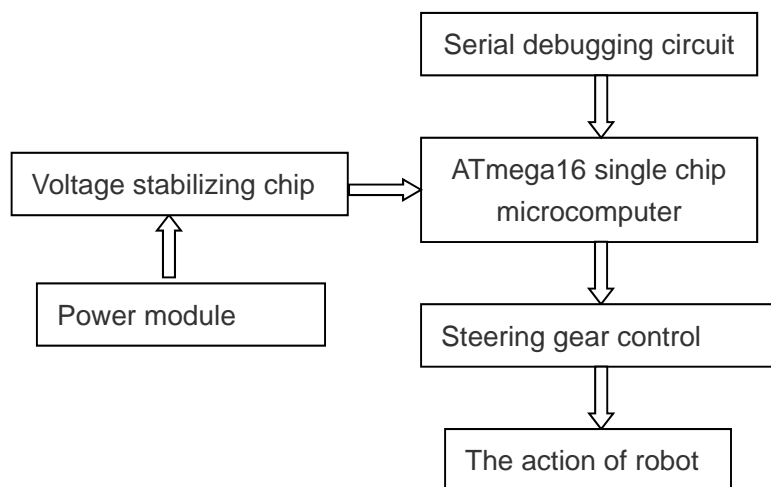


Fig. 1. The system structure diagram

### 3. The main hardware circuit

#### 3.1 Serial debugging circuit

The main controller of the circuit device is a MAXIM produced by MAX232MJE, the hardware interface simple, is a typical TTL--RS232 level conversion chip, IC chip contains two receiver and the driver chip, integrated with a power supply voltage converter, each receiver TIA/ EIA-232-F level conversion into 5V TTL/CMOS level, each transmitter to be converted into TTL/CMOS level to TIA/EIA-232-F level, the +5V power voltage transformation input is + 10V voltage RS-232C output level required. The practical application because MAX232 is sensitive to the noise of power, so it must be preceded by a decoupling capacitor between VCC and GND, and pay attention to the circuit board each capacitor connection, should be close to the MAX232 chip, to improve the anti-interference ability and the ability of data transmission in serial interface.

#### 3.2 The rudder control circuit

The steering gear is a kind of position servo drive, in the robot system can provide and maintain accurate angle control of [2], its working principle is: the control signal into the signal modulation chip by the receiver channel, get the DC bias voltage. It has an internal reference circuit, generating cycle is 20ms, the width is the reference signal of 1.5ms, compares the voltage of DC bias voltage and potentiometer gain, gain differential voltage output, is the positive and negative output voltage difference to the motor drive chip decided to motor. When the motor speed must, through the reduction gear drive cascading rotary potentiometers, the voltage difference is 0, the motor stops rotating. The control requirements as shown in figure 2.

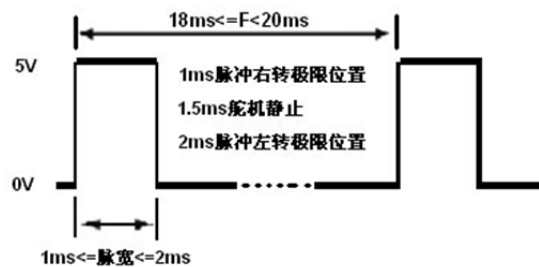


Fig. 2 Control steering requirements

Steering AVR MCU control with high precision, simple connection, and system reliability based on [3]. Using ATmega16 microcontroller as the control unit MG945 of the steering gear, the pulse width of the PWM signal to achieve changes in microsecond, so as to improve the precision of steering angle. The schematic diagram shown in figure 3.

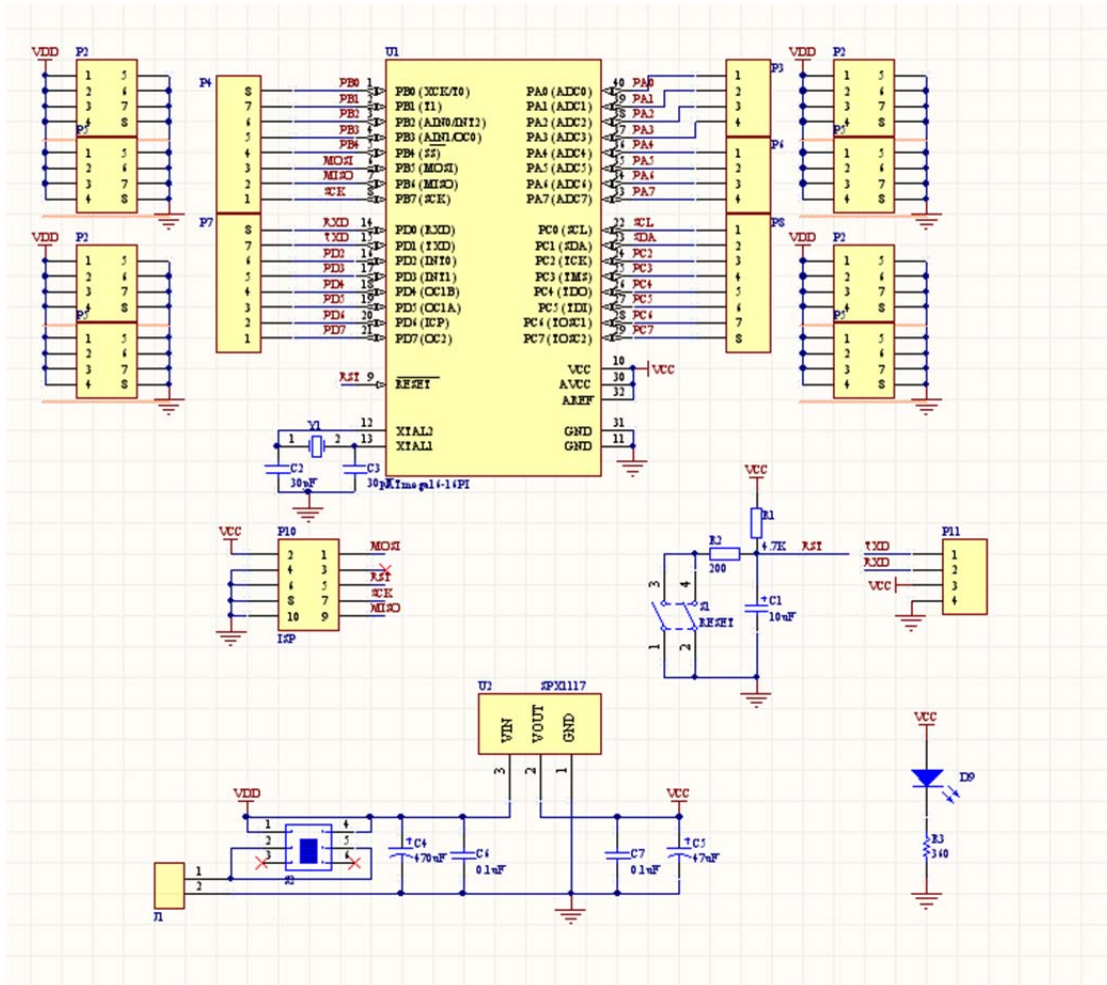


Fig. 3 Schematic diagram of servo drive

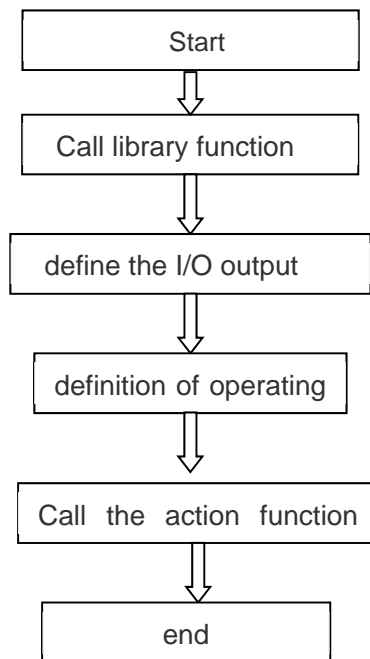


Figure 4 flow chart of main program

#### 4. Software design

The software of this system with the C language, the main program to complete the system hardware initialization, subroutine calls and other functions. The main program subroutine, action 5 is shown in Figure 4.

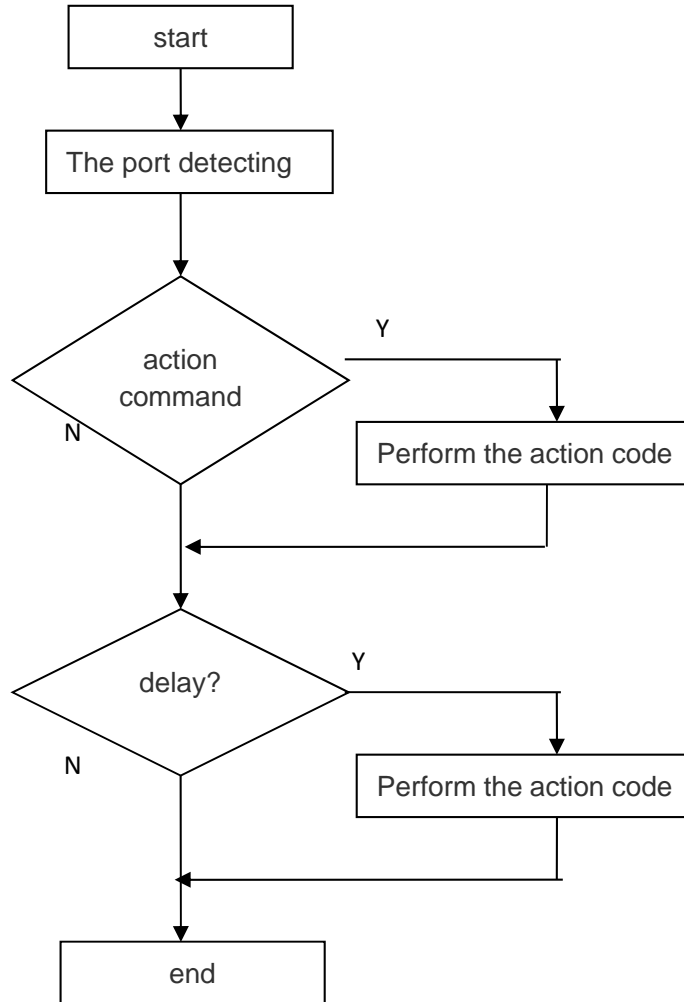


Figure 5 action subroutine flow chart

#### 5. Conclusion

The practice proved that, this paper designed the robot stable operation, graceful paper-cut, tasks and targets to achieve good results. Through the improvement of the robot hardware architecture, combined with the special debugging software that can realize the robot stability control of scissors independent performance of paper-cut art function.

#### Reference

- [1] 刘广瑞.机器人创新制作.西安:西北工业大学出版社,2007.
- [2] 陈继荣.智能电子创新制作—机器人制作入门.北京:科学出版社,2007.
- [3] 时玮.利用单片机 PWM 信号进行舵机控制.今日电子,2005,3:38-40.



# An Analysis of Influence Factor on Ideal Model Well Testing Curve

**Yang Chen**

College of Petroleum Engineering, Northeast Petroleum University Daqing 163318

## Abstract

Some carbonate formations with natural fracture, when fracture development is very flare out, and also exerts the characteristic of homogeneous reservoir. When it was developed with related hypotheses, and set up the well testing mathematical model for infinite homogeneous reservoir. Confirmed initial and terminal conditions. It can get bottom whole pressure formula of homogeneous infinite reservoir under the conditions that in view of well-bore storage coefficient and skin effect through Laplace transformation and numerical inverse. According to a certain of zero dimension well-bore pressure formula, it can draw well testing typical curve on homogeneous infinite reservoir, and also analyzes the influence factors on the basis of well testing curve characteristic analysis. So the conclusion is that the greater the well-bore storage coefficient ( $C_D$ ) is, the greater the differential of pressure peak is, and then downward sloping is steeper, as well the later the peak occurs. The greater the skin factor(S) is, and then the differential of pressure peak is greater. After the peak occurs, the downward sloping is steeper. The greater the  $C_D e^{2S}$  is, the higher the peak is, the downward sloping is steeper, and the time of occurring peak is later.

**Keywords:** Well testing curve; infinite homogeneous reservoir; mathematical model; influence factor.

## 1. Introduction

homogeneous reservoir Homogeneous reservoir is one of the most common types of strata, and the majority of sandstone formation in eastern China third lines often showed the characteristics of homogeneous reservoir. Some carbonate formations with natural fractures also exhibit characteristics of homogeneous reservoir when the crack growth is very uniform. Well test is a kind of effective and convenient technique to obtain the dynamic reservoir information, and the research of well test model is more mature and thorough. However, when a typical curve matching method is used to analyze data, parameter adjustment is often difficult, so rich and profound theoretical is needed foundation for more accurate interpretation. The study on the characteristics of homogeneous reservoir model of the pressure derivative curve showed that: at first pressure derivative is a straight line with an angle of 45 degrees, the downward sloping appeared after the peak value, and finally reached the 0.5 horizontal lines. Thus the peak should contain abundant reservoir information.

Research on the well test theory started abroad in twentieth Century 20's. In order to know the oil well production capacity, Mocre proposed analysis method of steady well testing in 1933, and this method is widely applied in twentieth Century thirty or forty's. In 1949, Van Everdingen published about the question of unstable seepage flow solved by using Laplace transform on AIME, marking the birth of unstable well testing analysis basis theory. In 1951 Horner proposed oil well pressure build-up test data analysis method basing on voltage degradation. This method has been widely used since it is presented. Later the development of MBH based MDH analysis method and Horner analysis method in the pressure

drop testing variable production well test analysis methods are improved and perfected the before method. These methods are the conventional well test analysis method.

In 1983, based on the Gringarten chart analysis method Boyd, raised the pressure derivative analysis method, this method enhances the type of oil and gas reservoir recognition function, and the pressure derivative chart and Gringarten chart are combined to form a composite chart a new well test analysis, the composite chart of modern well test analysis methods since its inception to the present widely use. With the development of seepage theory and computation technology, at present the analysis and Research on the theories and methods in the complex seepage numerical well testing has also made certain development

Yumen oil field well testing work in China started in twentieth Century 50 time, at that time, only some simple manometry and used for system for single well productivity well testing. In twentieth Century 60, is to understand the perfect wells into systematic well testing purposes and to formation pressure, flow coefficient and permeability for the purpose of pressure buildup test, through the introduction, absorption, digestion and development, current research in the field test technology and test analysis theory and method of our country has reached the international level.

## 2. Establishment and solution of a homogeneous reservoir mathematical model

### 2.1 Infinite homogeneous reservoir physical model

Well testing in homogeneous infinite formation, as shown in Figure 1, assume the following conditions:

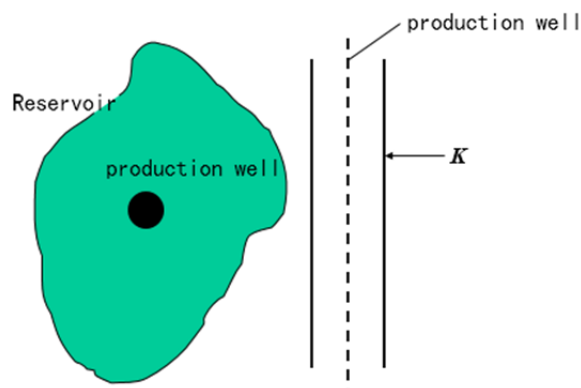


**Fig.1** Infinite homogeneous reservoir well testing model schematic diagram

- (1) single-phase slightly compressible liquid do radial percolation in reservoir;
- (2) ignoring gravity, capillary force;
- (3)  $r > r_w$  before the testing range throughout the mainland layer pressure as the initial reservoir pressure  $p_i$ ;
- (4) fluid flow satisfy the linear Darcy flow;
- (5) the wellbore flow considering the effect of wellbore storage and skin factor;
- (6) the formation of infinite thickness of reservoir, oil well to often yield  $Q$  production, testing is performed in the wells;
- (7) there is only one media formation, evenly distributed in the stratum.

## 2.2 A mathematical model of an infinite homogeneous reservoir

Before establishing the mathematical model, first introduce the following dimensionless quantity:

$$p_D = \frac{Kh(p_i - p)}{1.842 \times 10^{-3} q \mu B} \quad (1)$$

$$t_D = \frac{3.6Kt}{\phi \mu C_t r_w^2} \quad (2)$$

$$C_D = \frac{0.159C}{\phi \mu C_t h r_w^2} \quad (3)$$

$$r_D = \frac{r}{r_w} \quad (4)$$

According to the hypothesis and the theory of seepage mechanics in front, can set up the mathematical model, the seepage control equation:

$$\frac{\partial^2 p_D}{\partial r_D^2} + \frac{1}{r_D} \frac{\partial p_D}{\partial r_D} = \frac{\partial p_D}{\partial t_D} \quad (5)$$

Initial conditions:

$$p_D(r_D, 0) = 0 \quad (6)$$

The internal boundary condition:

$$p_{wD} = \left[ p_D - S \left( \frac{\partial p_D}{\partial r_D} \right) \right]_{r_D=1} \quad (7)$$

$$C_D \frac{dp_{wD}}{dt_D} - \left[ r_D \frac{\partial p_D}{\partial r_D} \right]_{r_D=1} = 1 \quad (8)$$

The outer boundary condition:

$$\lim_{r_D \rightarrow \infty} [p_D(r_D, t_D)] = 0 \quad (9)$$

## 2.3 Simplified analytical solutions of infinite formation reservoir mathematical model Laplace transform formula:

$$\bar{p}_D = \int_0^\infty p_D e^{-u t_D} dt_D \quad (10)$$

From (11) :

$$\frac{d^2 \bar{p}_D}{dr_D^2} + \frac{1}{r_D} \frac{d\bar{p}_D}{dr_D} = u \bar{p}_D \quad (12)$$

$$\bar{p}_D(r_D, \infty) = 0 \quad (13)$$

$$C_D u \bar{p}_{wD} - r_D \left. \frac{d\bar{p}_D}{dr_D} \right|_{r_D=1} = \frac{1}{u} \tag{14}$$

$$\bar{p}_{wD} = \left[ \bar{p}_D - S \frac{d\bar{p}_D}{dr_D} \right]_{r_D=1} \tag{14}$$

$$\bar{p}_{wD}(u) = \frac{1}{u \left[ u C_D + \frac{1}{S + \frac{K_0 \sqrt{u}}{\sqrt{u} K_1(\sqrt{u})}} \right]} \tag{15}$$

(11) can be transformed into Bessel equation:

$$r_D^2 \frac{d^2 \bar{p}_D}{dr_D^2} - r_D \frac{d\bar{p}_D}{dr_D} - u r_D^2 \bar{p}_D = 0 \tag{16}$$

The general solution form:

$$\bar{p}_D = A I_0(r_D \sqrt{u}) + B K_0(r_D \sqrt{u}) \tag{17}$$

By formula (15) requirements, available A=0 so

$$\bar{p}_D = B K_0(r_D \sqrt{u}) \tag{18}$$

K'0=-K1,so

$$\frac{d\bar{p}_D}{dr_D} = -B \sqrt{u} K_1(r_D \sqrt{u}) \tag{19}$$

Put (18) and (19) into (13) after finishing:

$$B = \frac{1 - C_D u^2 \bar{p}_{wD}}{u \sqrt{u} K_1(\sqrt{u})} \tag{20}$$

Put (18) and (19) into (14) after finishing:

$$\bar{p}_{wD} = B \left[ K_0(\sqrt{u}) + S \sqrt{u} K_1(\sqrt{u}) \right] \tag{21}$$

By formula (20) and (21) available

$$\bar{p}_{wD} = \frac{1 - C_D u^2 \bar{p}_{wD}}{u \sqrt{u} K_1(\sqrt{u})} \left[ K_0(\sqrt{u}) + S \sqrt{u} K_1(\sqrt{u}) \right] \tag{22}$$

Expression can be the bottom hole pressure on the Laplace space for

$$\bar{p}_{wD} = \frac{K_0(\sqrt{u}) + S \sqrt{u} K_1(\sqrt{u})}{u \left\{ \sqrt{u} K_1(\sqrt{u}) + C_D u \left[ K_0(\sqrt{u}) + S \sqrt{u} K_1(\sqrt{u}) \right] \right\}} \tag{23}$$

In the formula  $K_0(x)$ ,  $K_1(x)$  -- are zero valence, an order of imaginary argument Bessel function. (23) for the deformation can be:

$$\bar{p}_{wD}(u) = \frac{1}{u \left[ uC_D + \frac{1}{S + \frac{K_0\sqrt{u}}{\sqrt{u}K_1(\sqrt{u})}} \right]} \tag{24}$$

As the graph of the function  $S + \frac{K_0\sqrt{u}}{\sqrt{u}K_1(\sqrt{u})}$  can be used to approximate the semi log linear, so  $\ln \frac{2}{\gamma\sqrt{ue^{-2S}}}$ .

Then (24) can be written as:

$$\bar{p}_{wD}(u) = \frac{1}{u \left( uC_D + \frac{1}{\ln \frac{2}{\gamma\sqrt{ue^{-2S}}}} \right)} \tag{25}$$

And  $U = uC_D$

$$\bar{p}_{wD}(U) = \frac{1}{U + \left( \frac{1}{\ln \frac{2}{\gamma\sqrt{U/C_D}e^{2S}}} \right)} \tag{26}$$

Because the bottom hole pressure obtained above is Laplace space, so to inversion according to the inversion formula of Laplace space, following on the Laplace space of bottom hole pressure solution of inversion:

$$p_{wD}(t_D) = \frac{\ln 2}{t_D} \sum_{i=1}^N V_i \bar{p}_{wD}(S_i) \tag{27}$$

Among them,  $N$  is even,  $S_i = i \ln 2 / t_D$

$$V_i = (-1)^{\frac{N}{2}+1} \sum_{k=\frac{i+1}{2}}^{\min(i, N/2)} \frac{k^{N/2} (2k)!}{(N/2 - k)! (k - 1)! (i - k)! (2k - 1)!} \tag{28}$$

Principle that the algorithm in terms of  $N$  inversion formula of the larger, the more accurate calculation, but in the application due to rounding errors, the value of  $N$  is selected, the  $N$  in general

(6~18) even integer between.

### 3. Analysis of well test curve and its influence factors

According to the Laplace space derived from in front of the infinite homogeneous reservoir bottom hole pressure solution and its inversion formula corresponding, can program, get the curves of well test theory of infinite homogeneous reservoir.

#### 3.1 Analysis of the characteristics of an infinite homogeneous reservoir well test curve

Using the double log pressure derivative curve graph to represent the infinite reservoir characteristics of well test curve, as shown in figure 2:

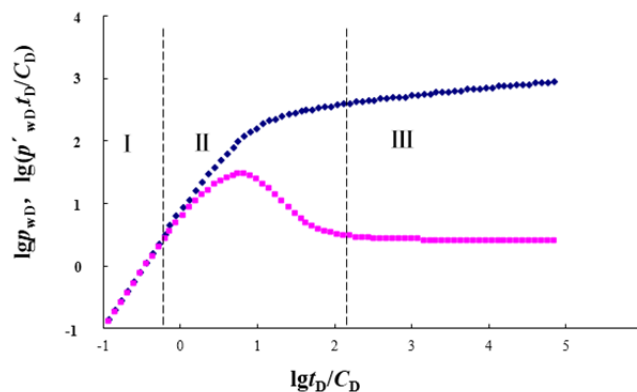


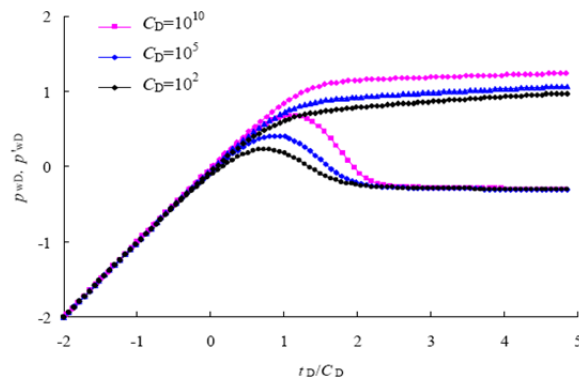
Fig.2 The well testing model typical curve of infinite homogeneous reservoir

Figure 2 is a typical double logarithmic characteristic graph recognition infinite homogeneous reservoir. It is shaped like a "two tooth fork", is divided into three stages.

The first stage is the "fork" part, in this section of the double logarithm of pressure and pressure derivative curve coincide, a linear 45 degrees, which indicates that the effect of stage is set pure wellbore storage effect. The second stage is the transition section; the pressure derivative peak appears after the downward sloping. The peak height, depending on the magnitude of  $C_D e^{2S}$ . In the parameters in group  $C_D e^{2S}$ ,  $C_D$  as the set of constant wellbore storage of dimensionless,  $S$  skin factor. Because the  $S$  value at index position, so the affected skin coefficient  $S$  value is bigger.  $C_D e^{2S}$  is bigger, then the higher the peak, down the steep peak, and the late time. The application of extremum method, can the relation  $C_D e^{2S}$  and the pressure derivative of the peak time of  $t_{max}$  :  $t_{max} = 1.1575 \lg C_D e^{2S} + 2.6789$ , so  $p'_{max} = 0.4273 \lg C_D e^{2S} + 0.4409$ . With the two formula can be seen, the pressure derivative peak trajectory is a straight line. Then the emergence of horizontal section in the third stage, which is the typical characteristic of producing radial flow in the formation, the pressure derivative curve showed 0.5 horizontal lines.

#### 3.2 The influence of wellbore storage coefficient $C_D$ of typical curve of well testing

We can see from Figure 3, in the  $S$  under the condition of invariable, changing the  $C_D$  value of the size, the bigger the  $C_D$  value, the peak of the pressure derivative is bigger also, along with the downward sloping is also steeper, and the peak time of the later [7, 8].



**Fig.3** The well-bore storage coefficient( $C_D$ ) impact on infinite homogeneous reservoir well testing typical curve( $S=100$ )

### 3.3 Effect of epidermal coefficient $S$ of typical curve of well testing

We can see from Figure 4 effect depends on the value of the parameter  $S$  in size, the bigger the  $S$  value, peak value of the pressure derivative is greater, and vice versa smaller. The larger the peak and the peak, after the more steep downward sloping. Figure 3 comparisons, effect of skin factor  $S$  on the model curve is much larger than the effects of the dimensionless wellbore storage coefficient  $C_D$  value of the model curve.

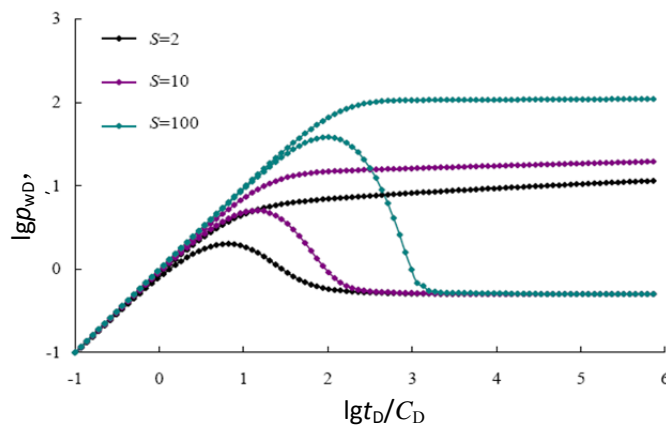


**Fig.4** The skin factor( $S$ ) impact on infinite homogeneous reservoir well testing typical curve ( $C_D=100$ )

### 3.4 Effect of $C_{De}^{2S}$ value on the typical curves of well test

The analysis of Figure 5, the peak height, depending on the size of the value of the parameter  $C_{De}^{2S}$ . The bigger the  $C_{De}^{2S}$  value, peak was higher, on the contrary, the less. And the peak, peak after the steeper sloped downward, and peak time than the later.

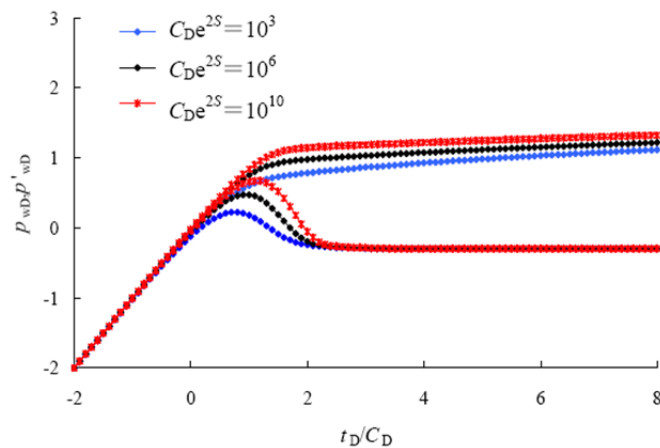


**Fig.5** variable values ( $C_D e^{2S}$ ) impact on infinite homogeneous reservoir well testing typical curve

#### 4. Conclusion

The wellbore storage coefficient  $C_D$  value is greater, the peak of the pressure derivative is greater also, along with the downward sloping is steep, and the peak time of the late, skin factor  $S$  value is greater, the greater the pressure derivative peak, peak appears after the more steep downward sloping. From Fig. comparison, effect of skin factor  $S$  on the model curve is much larger than the effects of the dimensionless wellbore storage coefficient  $C_D$  value of the model curve. The bigger the  $C_D e^{2S}$  value, peak was higher, on the contrary, the less. And the peak, peak after the more steep sloped downward, and peak time than the later.

#### Acknowledgement

This work is supported by the Major Projects of National Science and Technology of China: which serial numbers are 2011ZX05052-002-005 and 2011ZX05010-002-003.

#### References

- [1] Liao W X, Shen P P. Modern Well Test Analysis. Beijing: Petroleum Industry Press, 2002.
- [2] Ran X Q, Liao X W, et al. Extreme value study on well testing in homogeneous reservoir. Petroleum Exploration and Development, 2000,27 (1):67-68
- [3] Li X P, Zhang L H, Liu Q G. Well Test Analysis Method. Beijing: Petroleum Industry Press, 2009.
- [4] Ozkan, E, Raghavan, R. New solution for well-test-analysis problemspart1-analytical considerations. SPWFE, 1991, 9(2):359-368.
- [5] Qu GH, Chu Y, etal. Research on reservoir physical property changes of strong alkaline asp flooding. Science Technology and Engineering, 201212(18):4360-4362
- [6] Guohui Qu, Yikun Liu, Shengdong Jiang. Research on development factors affecting oil recovery of polymer flooding. Energy Education Science and Technology Part A: Energy Science and Research, 2013, 31(3):1787-1794.
- [7] Ozkan, E, Raghavan, R. New solution for well-test-analysis problemspart2-computational considerations and applications. SPWFE, 1991, 9(2):369-377.
- [8] Guohui Qu, Xingguo Gong and Yikun Liu. New research progress of the demulsification of produced liquid by polymer flooding. Journal of Chemical and Pharmaceutical Research, 2014, 6(1):634-640.



# Research on Moving Object Extraction Algorithms Based on Video Sequence

Li Cong<sup>1</sup>, Han Fei<sup>2</sup>

<sup>1</sup>School of science, Chang'an University, Xi'an 710064, Shaanxi, China

<sup>2</sup>School of science, Chang'an University, Xi'an 710064, Shaanxi, China

E-mail: <sup>1</sup>2392736250@qq.com

## Abstract

Moving target detection is basic of realizing task of object tracking, traffic monitoring and object behavior analysis. By computing the correlation coefficient of corresponding rows and ranks between two adjacent frames. Segment the moving object region by using the trait of target area which correlation coefficient is relative small. This arithmetic has the character of little calculating amount and not sensitive to the noise, it can be used to the multiple moving target detection under complication background. Experiments show that the algorithm can detect and separate all moving target accurately, and it is speed and reliable, so it fit for real time detection of moving targets.

**Keywords:** moving target detection; the correlation coefficient; image registration.

## 1. Introduction

The aim of movement detection is that depart variety area from background through the sequence image. Effective extraction of the moving object silhouette is essential for the subsequent processing, including target identification, tracking, behavior comprehension, and so on. But the irregular change of the background presents a range of challenges for the detection. So far, under the condition of the video camera fixed, the main motion objects detection algorithms include inter-frame subtraction method[1,2,3], three frames subtraction method [3,4,5],background subtraction method of Gaussian mixture model [4,5,6,7]and so on. Interface difference method is simple, but the detection is the part of the relative changes and no overlap was detected. Background difference is easy; this method is characterized by faster in calculation and high complexity of algorithms, so it is without practical value. Gaussian mixture model is to build the background model by multiple Gaussian distribution, thus it has strong scene adaptability, but its calculation speed is slow and the information is easily lost. In this paper, motion object region is extracted from the methods which calculate the correlation coefficient between the adjacent frames of gray-scale images. Experiments show that this algorithm is simple and easy realized, it is suitable for real-time processing.

## 2. Characteristics of video sequence

In the video sequence, image information is usually described in pixels, so the motion of the target is performance in the change of the pixel's values. In an ideal situation, between the two adjacent frames of the video sequences, the value of the pixels which have the moving target can change, while the backgrounds' can not change. So in the area which moving target exist, the correlation coefficient of rows and columns are small, and on the contrary, the rows and columns' correlation coefficient which

completely belong to the background are 1. But in reality, it will be influenced by the noise, some background part will change, their correlation coefficient close to 1.

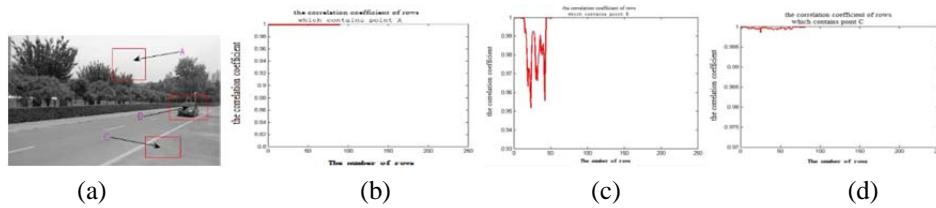


**Fig.1** Diagrams: (a) one frame of the video image (b) the correlation coefficient of rows which contains point A (c) the correlation coefficient of rows which contains point B (d) the correlation coefficient of rows which contains point C

### 3. The correlation coefficient

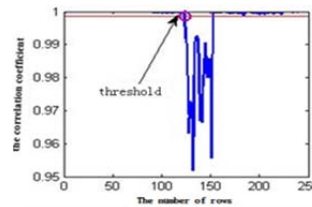
The correlation coefficient describes the linear correlation degree between two variables. Suppose you have two variables  $X, Y$ , then the formulas for correlation coefficients is as follows:

$$\rho_{X,Y} = \frac{\text{cov}(X,Y)}{\sigma_X \sigma_Y} ;$$

Among them, the value of  $\rho$  is between -1 to 1. If  $\rho > 0$ , it shows that two variables are related, if  $\rho < 0$ , it shows that two variables are negative correlation.



(a) one frame of the video image



(b) the threshold of the correlation coefficient

**Fig. 2** one frame of the video image and its threshold

Through the analysis of the characteristics of video sequence and the correlation coefficient, we can easily find the threshold; the position of the line in fig.2 (b) can be considered the threshold.

### 4. Moving target detection based on the correlation coefficient

By the characteristics of video sequence, we can remove the background using the method of calculate the correlation coefficient.

(1) Taking two adjacent frames in video sequences, recorded as  $A_k, A_{k+1}$ ,  $k$  is the frame order and  $1 \leq k \leq N-1$ ;

(2) Calculate the correlation coefficient of the rows and columns separately.

We assign a value of 0 to the rows and columns whose correlation coefficient are less than the threshold, and also assign a value of 1 to the rows and columns whose correlation coefficient are greater

than the threshold.

The results of the moving targets detection as fig.4:

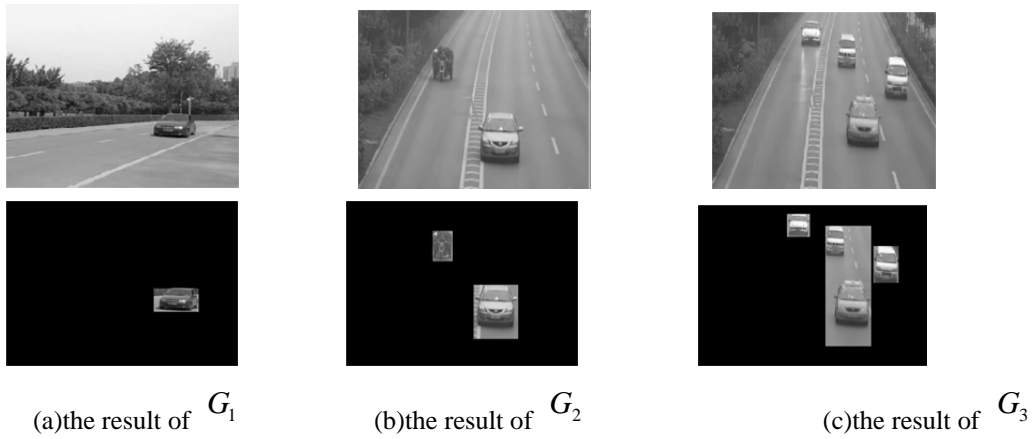


**Fig.4** one frame of the video image and their detect result

In the multiple moving target detection, calculate the correlation coefficient separately can effectively avoid detected out the redundant background, but for the area of the small part(as fig.6(b)),pixels are less, the result is not perfect by using the above method, so this paper use the method which calculate the correlation coefficient in block to detection the moving targets. This detection method is obviously.

### 5. Remove the background by the correlation coefficient in blocks

The idea of the blocks' correlation coefficient is divided the part which moving target in the adjacent frames into the same blocks, and then calculate the correlation coefficient of the corresponding blocks, it detect the moving target by using the characteristics that the blocks' correlation coefficients is small in the moving target areas. The histogram of blocks' correlation coefficient is as follows:

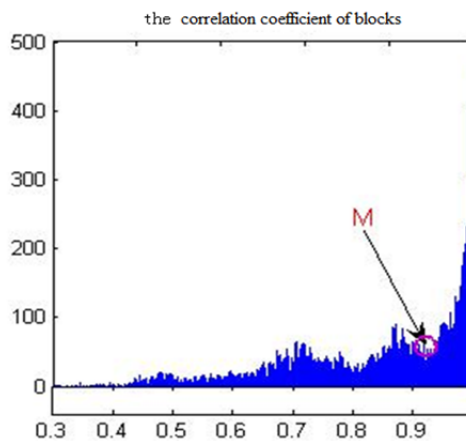


**Fig.7** The histogram of blocks' correlation coefficient

For the adjacent frames in video sequences, calculate the blocks' correlation coefficient ,we assign a value of 0 to the blocks whose correlation coefficient are less than the threshold, and also assign a value of 1 to the blocks whose correlation coefficient are greater than the threshold, then the moving target can be detected. The results of the moving targets detection by blocks' correlation coefficient are as fig.8:

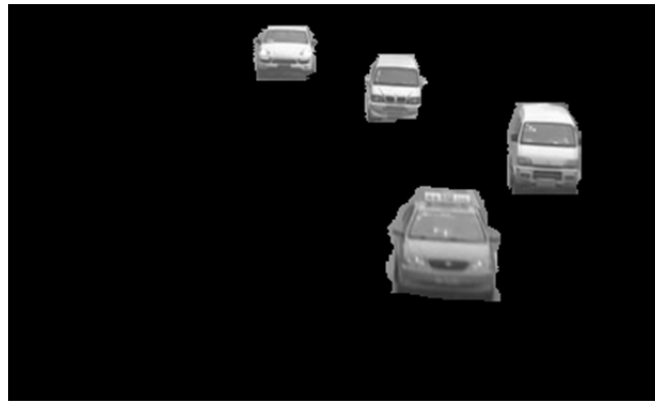


**Fig.8** The result of fig.4(c)

Above all, it is perfect to detect the moving target by using the method which calculates the correlation coefficient between two correlation coefficient, and the algorithm is stable.

### 5. The numerical experiments

The following is the moving target detection results using the method of Gaussian mixture method, background difference method and the method in this paper; the fifth column is the experiments which add noise to the third video sequence:

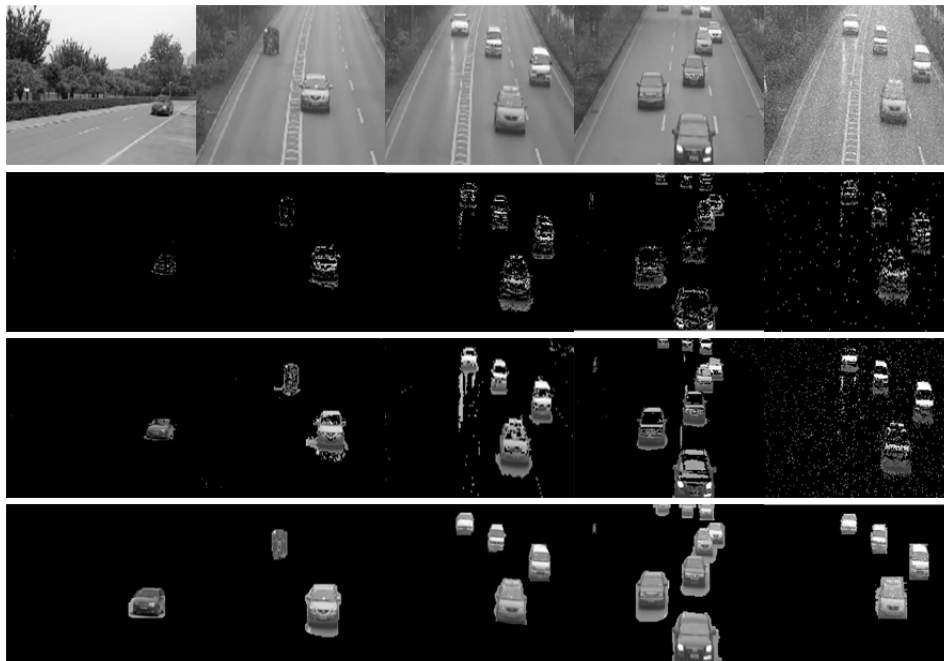


**Fig.9** The first line is one frame of the video image. The second line is the result of the detection by use the Gaussian mixture method. The third line is the result of the detection by use the frame difference method. The forth line is the result of the detection by use the background difference method, the fifth line is the result of the detection by use the method in this paper

From the experiments, we can see the method in this paper is superior to other methods and it is insensitive to noise.

## 6. Conclusions

In this paper, we detect the moving target by using the method of correlation coefficient, the result of the experiments are superior to other methods, and it is a basis for further study on moving target recognition ,tracking ,separation and so on. For more complex scenarios, we can combine with method of the rotate images or other methods; this will be the future study.

## References

- [1] Gan Ming-gang, Chen Jie. Moving Object Detection Algorithm Based on Three-Frame-Differencing and Edge Information. *Journal of Electronic & Information Technology*, 2010, 32(4):23-45.
- [2] XUE Li-xia, LUO Yan-lia, WANG Zuo-cheng. Detection algorithm of adaptive moving objects based on frame difference method. *Application Research of Computers*, 2011, 28(4) :1551-1554
- [3] LIU Xiao-ming, ZHANG Zhong-hui, LI Guan-yu, LV Ting-jie. Research on technology of traffic video incidents detection under highway condition[J]. *The Journal of China Universities of Posts and Telecommunications*, 2010(17):79-83.
- [4] LEE S, LEE J, HAYES M H. Adaptive background generation for automatic detection of initial object region in multiple color-filter aperture camera-based surveillance system, *IEEE Trans on Consumer Electronics*, 2012, 58(1): 104-110.
- [5] Li Hong, Yang Ting-wu, Ren Pu-zhou, Li Zhao-hui. Moving target trackong based on optucal flow field analysis in complex background. *Opto-Electronic Engineering*, 2006, 33(10):13-17.
- [6] ZHAO Long, HE Xin-hua. Adaptive gaussian mixture learning for moving object detection. 2010 3rd IEEE International Conference on Broadband Network & Multimedia Technology, 2010(3):2-7.
- [7] Gauglitz S, Hollerer T. Evaluation of interest point detectors and feature descriptors for vidual tracking. *International Journal of Computer Vision*, 2011, 94(3): 335-360.
- [8] Li Ming-zhi, Ma Zhi-qiang, Shan Yong. Adaptive background update based on Gaussian mixture model under complex conditon. *Journal of Computer Applications*, 2011, 31(7):1831-1834.
- [9] LI Ming, ZHAO Xun-jie. Improved moving objects detection algorithm based on Gaussian mi-xture model. *Computer Engineering and Applications*, 2011, 47(8):204-206.



# The Construction of Digital Campus Based on City Engine

Chao Hui<sup>1</sup>, Ge Xuewen<sup>2</sup>, Jin Feng<sup>3</sup>, Lin Bo<sup>4</sup>, Shi Yali<sup>5</sup>

<sup>1,2,3,4,5</sup>Hebei United University, China

<sup>1</sup>Corresponding author

**E-mail:** <sup>1</sup>*hchao@heuu.edu.cn*, <sup>2</sup>*1165494518@qq.com*, <sup>3</sup>*649658350@qq.com*, <sup>4</sup>*1362072650@qq.com*,  
<sup>5</sup>*1973273763@qq.com*

## Abstract

On the base of the research of CGA language, we have carried on the preliminary build to the building using City Engine platform. By comprehensive analysis of CGA, on the basis of 3 d modeling language, for example, we use CGA language to build digital campus of Hebei united University of joint three-dimensional system.

**Keywords:** City Engine, 3 d Modeling, CGA, ArcGIS.

## 1. Introduction

City Engine is the software developed by Esri company for three-dimensional city modeling , it is mainly used in Digital city、city planning、rail transit、electric power、line pipe、building trade、national defense、emulation、development of games、film production and other fields. City Engine can use 2D shp data quickly create 3D scene, and efficient planning design[1-2] .The perfect support for ArcGIS make existing base of GIS data can be quickly implemented does not need to convert three-dimensional modeling, reduce the cost of investment in the system., and the modeling period of the GIS system is shortened. Esri City Engine promote the 3D modeling capabilities of ArcGIS, full use of GIS data quickly create 3D content, provide safeguard for the ArcGIS's 3D data acquisition, make the ArcGIS has the more perfect solution to 3D[3] . This research mainly based on the campus of Hebei United University as the study area, use CGA rule, build 3D campus system, can realize 3D campus landscape、query function and so on.

## 2. The introduction of the system related technology

CGA is the standard City Engine software modeling language belonging to ERSI company, CGA is Computer Generated Architecture, CGA Shape Grammar is a special programming language belonging to City Engine software, this language is used to generate 3D building model<sup>[4]</sup> .As a new member of modeling language, CGA language can fully support the ArcGIS, and can quickly use 2D data to create 3D scene. The thoughts of Semantic modeling are to define the rules, through iterative refinement design to create details and complete content. These rules operating are composed of geometric shapes, these make a lot of existing basic GIS data(like parcel area、 structure、 Urban road centerline etc) can be used directly without convert, in order to realize rapid 3D modeling, reduce the cost of reinvestment, so CGA language can batch modeling.

## 3. Hebei United University campus system design

### 3.1 The system overall design scheme

The aim of designing this system is to achieve campus 2D, 3D information browsing, roaming, attribute query, elements query and the function of data update. The concrete design scheme as figure 1 shown:

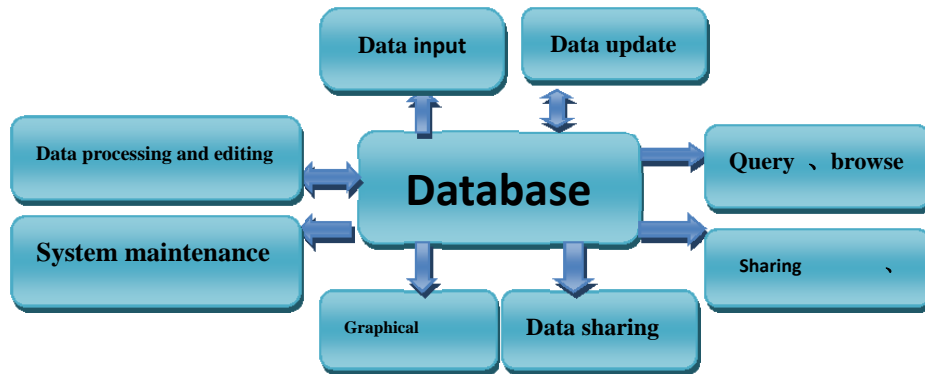


Fig.1 .The system overall design scheme

### 3.2 The concrete modeling plans to model different ground features respectively.

There are varieties of modeling methods for different ground features, for example, the simulation of the terrain, mainly use Triangle Irregular Net(TIN) data model which generated by vector data to generate the terrain surface, provide a simulate surface<sup>[7]</sup> for other ground features; The important and complex ground features, such as complicated teaching buildings, the door of teaching building, benches and something symbolic, use these modeling tools, like Ketchup and 3D Max to model, then through writing rules of CGA, developed by City Engine components to lead 3D models into 3D scenes, as shown in figure 2 of building the comprehensive teaching building and the fountain.



(a) the comprehensive teaching building

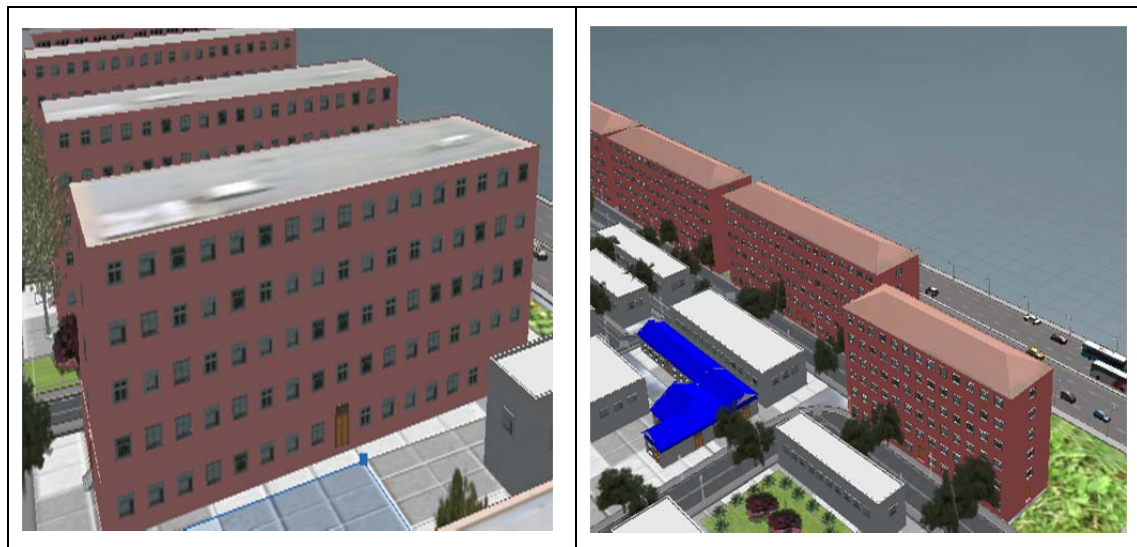
(b) the fountain

Fig.2. Complex and ordinary ground features

For the universal ground features which are in low height, such as the lawn, lakes, highway, court, etc., use the surface texture load module based on City Engine's component development, in this way we can realize 3D modeling for low ground features<sup>[7-9]</sup>. For the ground buildings of quantity, very similar,



simple appearance, such as the buildings look like cuboids or have herringbone houstops, especially the students' apartments and architectural complex. Use the CGA rules based on City Engine to modeling these ground features of the above, as shown in figure 3, these students' apartments and experimental base are all batch modeling.



(a) The students' apartments

(b) Architectural complex.

**Fig.3.** Batch builds similar buildings

### 3.3 The process of making model

3D modeling is based on City Engine software, this software can realize the reconstruction of the true 3D landscape, it also support the map data generated by ArcGIS, 2D map data can be imported into the software in order to create profile model, then do the preliminary optimization to details of the model, stretch and map processing, try to approached to the real scene. City Engine mainly use rules for modeling that can adopt external built model by establishing rules of CGA file in advance. The main process is as follows:

#### 3.3.1 Basic data acquisition.

1. Elevation data: Hebei United University digit 30m elevation data GDEM;
2. Terrain texture data: use Get screen, combining with Google maps intercept appropriate height and proper resolution as campus texture map;
3. Land use type vector data: Use Arc Map to load the terrain texture, highlight by hands, complete the vector, get the SHP format, and convert the format to GDB in the Arc Catalog.

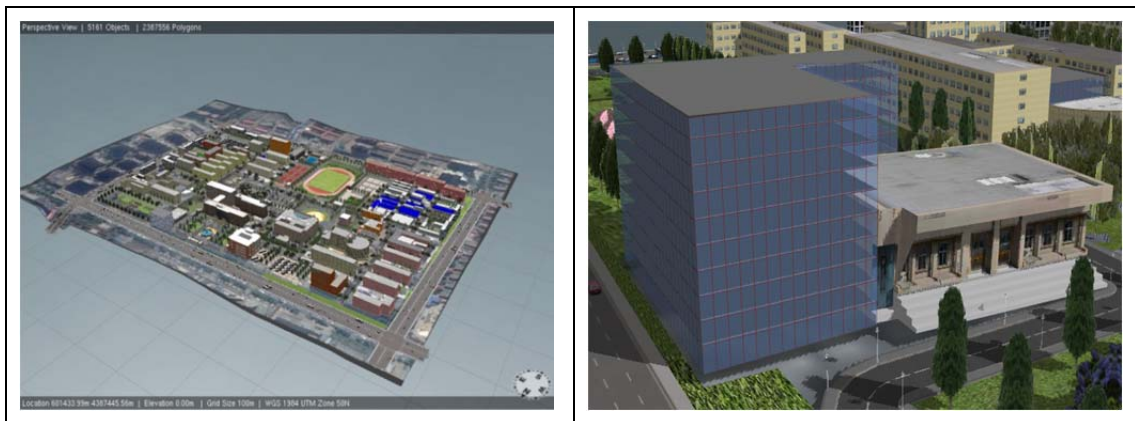
#### 3.3.2. Model making.

1. Use cityengine2012 to load DEM and texture, then load the data of GDB and paste them in together;
2. The specific modeling process: There are three kinds of modeling methods in this modeling process: by writing CGA rules, manual stretching and modeling by façade wizard. Among the three methods, CGA is taken as the principal methods, specific rules files are in the rules folder;

## 4. System implementation

#### 4.1 Background information

Modeling area is the main campus of Hebei United University, it turns out to be Hebei Polytechnic University headquarter which covers an area of 750000 square meters, construction area is more than 190000 square meters, the whole school buildings are built after the earthquake, base maps of this concrete model is as shown in figure 4. In the 21<sup>st</sup> century, the Library、the Fifth teaching building and the new Chemical lab building have been built in succession, but the campus has coordinated in the whole architectural features. The main campus has the famous earthquake ruins which are one of the national key protective earthquake ruins, it still retains the original earthquake after 30 years of wind and rain, so the earthquake ruins become the representative of the school buildings.



(a) The base map of Hebei Unity University

(b) The auditorium of Hebei Unity University

**Fig.4.** An aerial view of Hebei Unity University campus

#### 4.2 The introduction of campus 3D system function

In this study, the Hebei Unity University campus and the surrounding environment make good examples, in order to build digital campus 3D landscape system based on City Engine. It has realized functions of the display for 3D campus model, roam in image, brows the spatial information, query and analysis of attribute information. The next part contains the function of system each module respectively.

##### 4.2.1 3D campus scene roaming

On the base map, use the CGA language to build 3D campus structures so as to realize roaming in image, just as the Hebei Unity University's new restaurant in the figure 5(a), mainly adopt map processing to build; The figure5 (b) is Hebei Unity University's experiment center; The figure5(c) is the library of Hebei Unity University; The figure5 (d) is the Front Gate of Hebei Unity University.

##### 4.2.2 Spatial properties data query

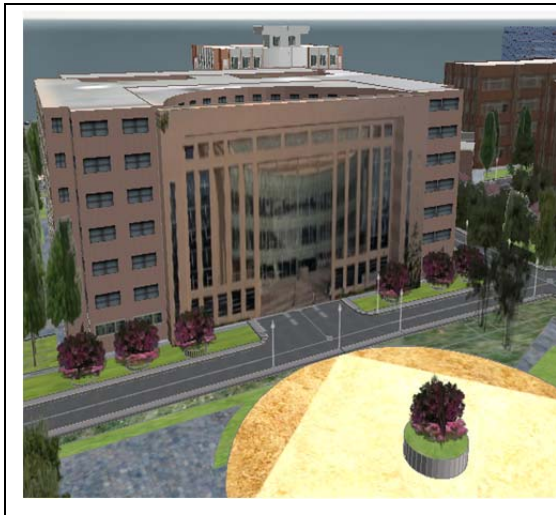
The system can provide the spatial properties data query service, choose target ground features in the project to view the elevation data of the model or make a property lookup based on the ground features in the base map, as is shown in figure 6.



(a) Hebei Unity University's new restaurant



(b) Hebei Unity University's experiment center



(c) The library of Hebei Unity University



(d) Front Gate of Hebei Unity University.

Fig.5. 3D scene



Fig.6. Attribute query



#### 4.2.3 Measurement and analysis

The system provides a simple 3D measuring function; users can select the target ground features to measure the length of it, as is shown in figure 7.



**Fig.7.** Distance measurement

#### 5. Concluding remarks

On the basis of CGA language, this article uses City Engine as supporting platform to design and realize constructing a 3D digital campus system of Hebei Unity University. The display of this system based on City Engine is simple, fast and beautiful, in addition, 3D imaging technology has advanced interaction and authenticity. At present, this system has achieved the preliminary desired effect, realize the function of 2D/3D map browsing, query and spatial analysis etc, this system is interactive and clear. 3D campus model can optimize the leadership and management system with its intuitive properties, in favour of highly centralizing, configuring and interacting campus planning information.

#### Reference

- [1] Gaoshangyu. The design and implementation of digital campus information system based on GIS. Shandong University of Science and Technology, 2005.
- [2] Yangwunian, Puguoliang, Yudaijun, etc. Construction and implementation of digital campus of Chengdu University of Technology of spatial information system. Journal of Chengdu University of Technology: Natural Science Edition, 2005, 32(1) : 101-106.
- [3] Wang Yan. Chengdu University of Technology Digital Campus project preliminary design of Chengdu University of Technology, 2002
- [4] Zhongguangzhi. ArcGIS Flex API WebGIS design based on. science of Surveying and mapping, 2012,37 (3): 147-149.
- [5] Shaomingxu, Xuhui ping, Tanrufu., etc. Design and implementation of virtual campus 3D linkage. Geographic information world, 2008,6 (2): 74-75.
- [6] Huangxingyuan, Majinsong. Introduction to geographic information system. Beijing: Higher Education Press, 2008
- [7] Huliangno, Wangzhihong, Hanliqin, etc. Construction and application of 3D virtual campus network. Science of Surveying and mapping, 2013 (1): 168-170.

- [8] Wupuzhou, Majinhai, Weihaiyan, etc. Design and implementation of the campus WebGIS system ArcGIS based on Server Remote sensing information, 2007 (2): 77-81.
- [9] Esri (Chinese) Information Technology Co., Ltd.. CityEngine Chinese tutorial.
- [10] Wuyuxiao, Chenjing, Linhuan. The design and implementation of digital campus GIS system based on JAVARemote sensing information, 2004 (1): 46-48.
- [11] Xuhanwei, Rudezhu, Hejiang. Research on three dimensional GIS function development technology based on ArcEngine. Engineering of Surveying and mapping, 2006,15 (6): 50-54.
- [12] GGongjianhua, Linhun, Tanqian. Design and experiment of virtual campus of Chinese University Hong Kong 2002 Journal of Surveying and mapping, 31 (1): 39-43.
- [13] Chenyingxiang. Application of 3D GIS modeling and visualization technology. Wuhan University of Technology, 2007.



# Research of Main Arch on Stone Arch Bridge Reinforcement Engineering's Construction Monitoring

Hui Yu<sup>1</sup>, Liang Tang<sup>2</sup>, Zhixiang Zhou<sup>3</sup>

School of Architecture and Civil Engineering, Chongqing JiaoTong university

<sup>3</sup>Corresponding author

## Abstract

Construction monitoring in bridge construction and reinforcement is an essential part of the reconstruction project. Monitoring the linear deflection and stress of the bridge make it possible to solve problems in time, and to ensure consistent with the design. According to the background of Da Xi He No. 3 bridge reinforcement project and combined with the design scheme of reinforcement and reconstruction, this paper expounds the construction monitoring technology and effect on the linear and stress monitoring.

**Keywords:** stone arch bridge, main arch, reinforcement, linear, stress, construction monitoring.

## 1. Introduction

Arch bridge is widely used in highway for beautiful shape, pass-over capacity and can fully make use of material strength. Stone arch bridge, as a kind of arch bridge, has been built long ago and appears a lot of diseases. With the bearing capacity decreasing, unsafe bridge will cause accidents and endanger the people's lives and property. The period of days spend on constructing a new bridge is longer. It will cost enormous amount of money and certainly cause the traffic interruption for months. Therefore, it seems the bridge reinforcement is one of the best choices. To ensure the construction quality and constructing the bridge safely, the construction of monitor is essential in the reinforcement construction process[2]. Based on the background of DaXiHe No. 3 bridge reinforcement project, this paper offers reference for similar bridge construction monitoring by introducing deformation monitoring and stress monitoring method.

## 2. Project summary and reinforcement methods

### 2.1. Project summary

DaXiHe No. 3 bridge is a stone arch bridge, located in Fuling, a district belong to the city of Chongqing in China. It is 90 meters long (including two of 30m of vice-arches and 60 meters of main arch) and 20 meters wide (including 6.8 meters of traffic lanes and 0.75 meters of pavement on each side). The arch axis of main arch utilizes the catenary curve. The net span of main arch is 60 meters and rise is 11.25 meters. The rise to span ratio is 0.1875. The net span of spandrel arch is 4 meters and rise is 1 meters. The rise to span ratio is 0.25. The bridge deck system is 1.2%. The layout of the bridge is shown in figure 1.

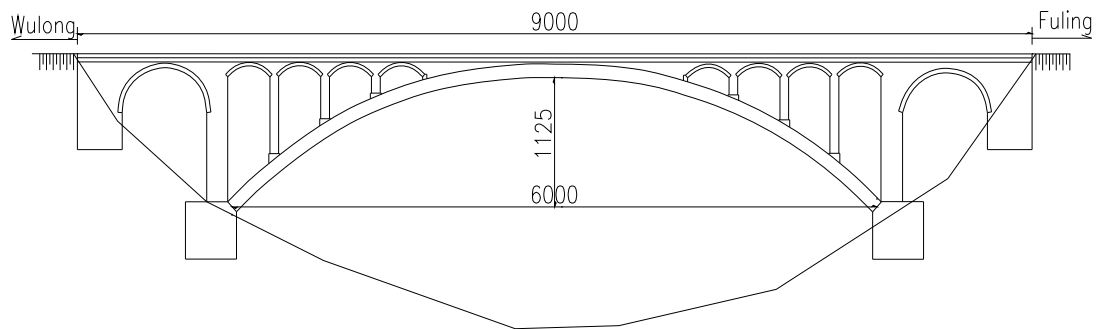


Fig. 1. The layout of DaXiHe No. 3 bridge (unit: mm)

## 2.2. The scheme of the reinforcement design of the main arch bridge

In this paper, the main arch reinforcement is studied. To minimize the damage of the original structure, simplify the reinforcement structure, safe and convenient construction, the main arch was reinforced by C-S-C (concrete-stone- concrete) method.

(1)The filled spandrel of main arch: Under axial pressure and positive bending moments, which is easy to appear the over- tensile -stress on lower limb under the most unfavorable effect combination. Hence the filled spandrel of main arch reinforcement can adopt l-shaped reinforced concrete arch rib as an auxiliary of the original stone main arch stress, and reduce the trouble and risk of dismantling construction on the filled spandrel of main arch. l -shaped reinforced concrete arch rib is shown in figure 2.

(2)The open spandrel of main arch: Under axial pressure and negative bending moments, and it is easy to appear the over- tensile -stress on upper limb under the most unfavorable effect combination. Hence the filled spandrel of main arch reinforcement can adopt trough type reinforced concrete arch rib as an auxiliary of the original stone main arch stress. Trough type reinforced concrete arch rib is shown in figure 3.

(3)It is essential to set transverse struts between left and right through type reinforced concrete arch rib with the appropriate spacing in the corresponding position of cross wall and cross section. It greatly improves the integrity of bridge.

(4) The trough type reinforced concrete arch rib in the foot is joined to the reinforced concrete abutment; subsequently a new framework of reinforced concrete arch ribs is formed.

The new concrete structure works together with the stone structure which mainly relies on the compatibility of deformation. It increases the area of section and the moment of inertia and decreases the stress of the original stone arch [3]. The main arch reinforcement improves bearing capacity. The reinforced main arch is shown in figure 4.



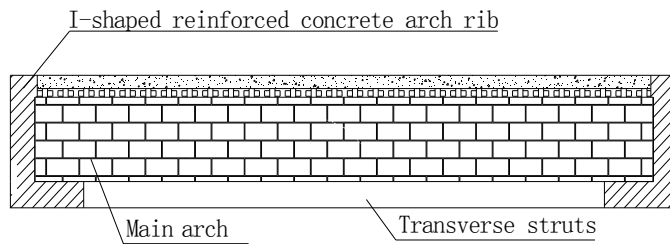


Fig.2. I-shaped reinforced concrete arch rib.

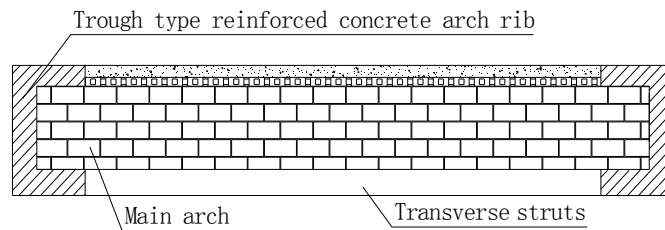


Fig. 3. Trough type reinforced concrete arch rib.

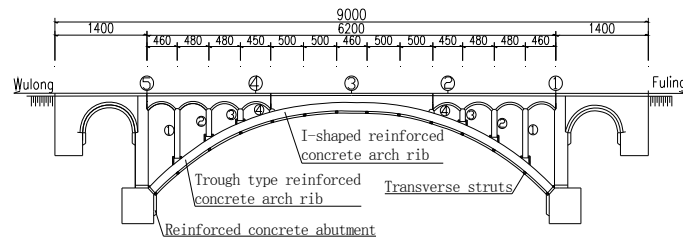


Fig.4. The elevation of reinforced main arch (unit: mm)

### 3. Deformation monitor

The observation data of deflection and plane position is an important content during its construction. Ensuring the process of bridge reinforcement is safe. To reduce the influence of other factors as far as possible, the observation data of deflection and plane position should be measured in the low temperature (in the morning before the sun come out).The temperature should be recorded at the same time[4]. The effects of main construction steps on displacement can be reflected by deformation monitor.

#### 3.1. The selection of deformation monitoring location and measurement method

The monitor points corresponding to main control sections (vault, arch foot, L/4) on the main arch should be chosen in the upstream and downstream of bridge deck. The monitor points are shown in figure 4. In the upstream of bridge deck, the base point is 1#.The monitor points of arch foot is 2# and 6#. The monitor points of L/4 of main arch are 3# and 5#. The monitor points of vault are 4#. In the downstream of bridge deck, the base point is 7#.The monitor points of arch foot is 8# and 11#. The monitor points of

L/4 of main arch are 9# and 12#. The monitor points of vault are 10#. Steel rules ought to be set up at each monitor points by a certain elevation [5]. The deformation of bridge deck is measured by relative level of elevation. The change of elevation between twice measurements is the deformation of main arch between twice measurements.

### 3.2. The selection of deformation measurement

As a result of long span of main arch, large amount of concrete volume and difficult construction, the concreting of main arch was divided into five times to complete. The first concreting is from arch foot to the first cross wall. The second concreting is from the first cross wall to the second cross wall. The third concreting is from the second cross wall to the third cross wall. The fourth concreting is from the third cross wall to the fourth cross wall. The fifth concreting is on the filled spandrel of main arch. Each concreting is symmetrical construction. Each time before and after the concreting is essential stage of construction, starting from the beginning of the main arch reinforcement.

### 3.3. The comparison for deformation measurement data and model data

In advance of the main arch reinforcement, the initial data was measured. The next step is measure deformation many times as soon as possible as it is a vital stage of construction. The construction should be shut down and analyze the outcome for the incident when the deformation measurement data has change dramatically.

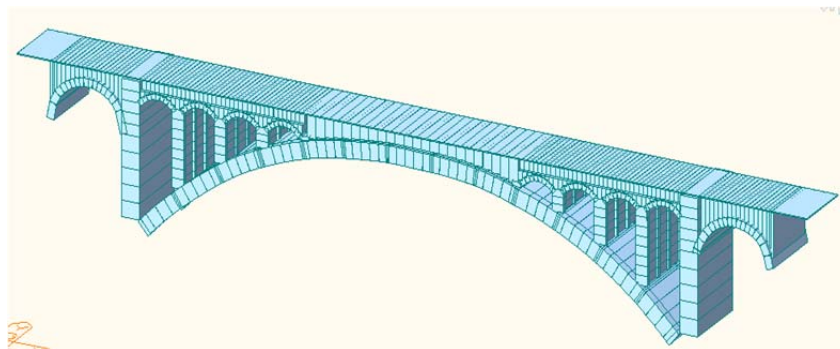


**Fig.5.** The model of main arch reinforcement of DaXiHe No. 3 bridge.

The model used to simulate the every important construction process should be built before the measurement of main arch reinforcement. This bridge is modeled by the finite element software Midas Civil and by using beam element. The whole bridge model is a total of 744 nodes, 592 units [6]. The model is shown in figure 5.

The construction stage joint interface method is used to simulate the process of main arch reinforcement. Firstly, the main arch section at each construction stage should be confirmed. After that, every stage of construction should be built. Then the new concrete section should be activated in suitable construction stages. So the original stone main arch and the new concrete arch rib are combined into a new main arch. Based on the stiffness of two kinds of components and the principle of deflections consistency, the internal force and stress of new main arch is distributed. Besides the shrinkage and creep caused by different material age should be taken into consideration [7]. The relative elevation can be

calculated by dealing with model data, and then compare model data and measurement data. The measurement data is shown in table 1. The model data is shown in table 2.

**Table 1.** The measurement data of deformation of main arch reinforcement-relative elevation (unit: mm).

Monitor point	Condition	Before the	The first	The second	The third	The fourth	The fifth
		main arch reinforcement	concreting	concreting	concreting	concreting	concreting
Base point1	1	t					
Arch foot of Fuling	2	2.2	2.3	2.3	2.3	2.2	2.2
L/4 of Fuling	3	5.7	5.7	6.1	5.9	5.9	5.8
Vault	4	8.9	8.6	9.2	9.5	8.9	9.4
L/4 of Wulong	5	5.8	5.8	6.4	6.1	6.1	6.4
Arch foot of Wulong	6	1	1.1	1.1	1.2	1	1.3
Base point	7						
Arch foot of Fuling	8	5	5.2	5.3	5	4.9	4.8
L/4 of Fuling	9	8.7	8.8	9.1	8.6	9	8.9
Vault	10	10.9	11	11.4	10.6	10.9	11.1
L/4 of Wulong	11	6.9	7.1	7.5	6.9	7.1	7.1
Arch foot of Wulong	12	4.2	4.2	4.4	4.3	4.2	4

Note: "L" stands for the length of main arch. the same below.

**Table2.** The model data of deformation of main arch reinforcement-relative elevation (unit: mm).

Monitor point	Condition	Before the	The first	The second	The third	The fourth	The fifth
		main arch reinforcement	concreting	concreting	concreting	concreting	concreting
Base point1							
Arch foot of Fuling		1.201	1.21	1.237	1.267	1.28	1.239
L/4 of Fuling		7.32	7.329	7.447	7.787	8.137	8.754
Vault		11.593	11.296	10.38	9.759	9.395	13.981
L/4 of Wulong		6.77	6.804	6.973	7.313	7.594	8.013
Arch foot of Wulong		0.887	0.903	0.948	0.99	1.001	0.923

It is indicate that vault is the most liable to deform in the process of reinforcement after comparing the measurement deformation data and the model data of main arch reinforcement. It is followed by part L/4. Subsequently; the deformation of arch foot is extremely small. Considering the precision of level and steel rule, temperature, wind speed, the manual measurement error and other factors, it is inevitable for the difference between the measurement data and the model data. In general, the change trend of

measurement data is consistent with the change trend of model data, besides the change of measurement data is hold within modest bounds.

#### 4. Stress monitoring

##### 4.1. The selection of stress monitoring location and measurement method

Considering cost of the monitoring, it is impossible for each section of all the components to monitor stress. In general, the monitors are specifically buried on the critical sections so that the critical control sections could take place of all control sections [8]. Consequently, the stress state of the entire bridge could be controlled on the whole and get the most valuable information at cost savings. The sections of stress data acquisition are mainly at arch foot, L/4 and vault in main arch which are in a high stress area or repeated stress area and which are the most easily broken. They are most representative for security status and the most sensitive to precursor information of potential risk [9].

The equipment of stress monitoring is vibrating wire sensors which reflect stress of construction by the change of frequencies. The vibration frequency will be altered followed by the change of the distance between the two endpoints under changed load. The stress increment measured will be accurately calculated though the change of vibration frequency. Vibrating wire sensors with characteristics of high precision and small size which have been widely used for monitoring the safety of bridge [10]. What calls for special attention is that the measurement of stress data is controlled within 3hrs before sunrise in order to avoid the influence of temperature. The layout of vibrating wire sensors is shown in figure 6.

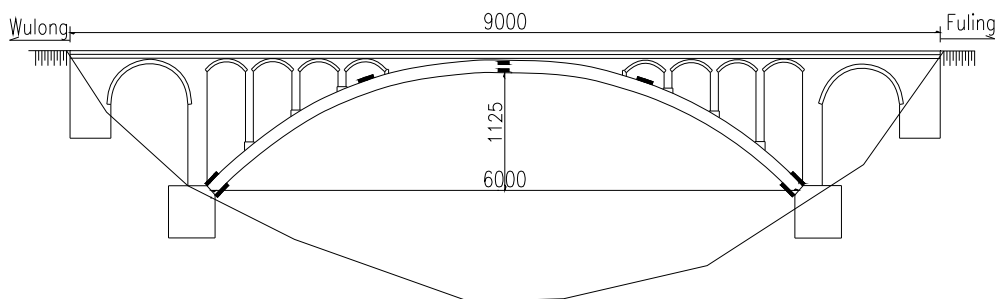


Fig.6. The layout of vibrating wire sensors

##### 4.2. Comparison of the stress measurement data with the stress model data

The stress value on each construction stage can be searched in the output of the main arch reinforcement model. Plus the change of stress on critical control sections on each construction stage can be forecasted. Therefore the model data provide strong support for safety control in construction and construction technology and quality. Receiving the initial data before the measurement of main arch reinforcement, and then measure stress data many times as soon as possible in important construction stages. The construction should be shut down and analyze the results of the incident when the stress data of measurement has changed dramatically [11]. The stress data of measurement is shown in table 3.

**Table 3.** The stress measurement on each construction stage (unit: MPA)

Condition Monitor point	Before the main arch reinforcement	The first concreting	The second concreting	The third concreting	The fourth concreting	The fifth concreting
Upper limb of arch foot of Wulong	-0.5004	-0.60048	-0.63384	-0.70056	-0.70056	-0.76728
Lower limb of arch foot of Wulong	-0.90072	-0.96744	-1.03416	-1.06752	-1.03416	-1.1676
L/4 of Wulong	-0.6672	-0.70056	-0.76728	-0.73392	-0.6672	-0.76728
Upper limb of vault	-0.834	-0.6672	-0.76728	-0.80064	-0.80064	-0.73392
Lower limb of vault L/4 of Fuling	-1.16792	-1.16784	-1.1012	-1.16792	-1.16792	-1.13432
Upper limb of arch foot of Fuling	-0.43352	-0.5004	-0.43368	-0.5004	-0.46704	-0.73392
Lower limb of arch foot of Fuling	-0.60048	-0.63384	-0.70056	-0.63384	-0.70056	-0.80064
	-0.93408	-1.23432	-1.23432	-1.3344	-1.3344	-1.26768

Because of the model being built by using beam element in Midas Civil, the stress of beam element in output are just the cross-section mean stress. Whatever the stress value of beam element in construction stage or the stress value of beam element in completion stage should be searched in the table of analysis results. The stress data of model is shown in table4.

**Table4.** The stress of model on each construction stage (unit: MPA)

Condition Monitor point	Before the main arch reinforcement	The first concreting	The second concreting	The third concreting	The fourth concreting	The fifth concreting
Arch foot of Wulong	-1.35	-1.37	-1.38	-1.4	-1.42	-1.51
L/4 of Wulong	-0.994	-0.996	-1	-1.02	-1.06	-1.12
Vault	-0.946	-0.948	-0.957	-0.977	-0.99	-1.12
L/4 of Fuling	-0.982	-0.983	-0.991	-0.101	-1.05	-1.11
Arch foot of Fuling	-	-1.39	-1.4	-1.42	-1.44	-1.54

In order to be convenient to view the change of stress on main control sections, five broken line graphs are made. They are shown in figure7-11.

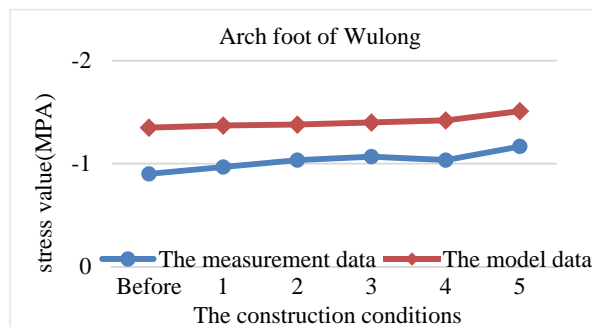


**Fig.7.** The change of stress on arch foot of Wulong

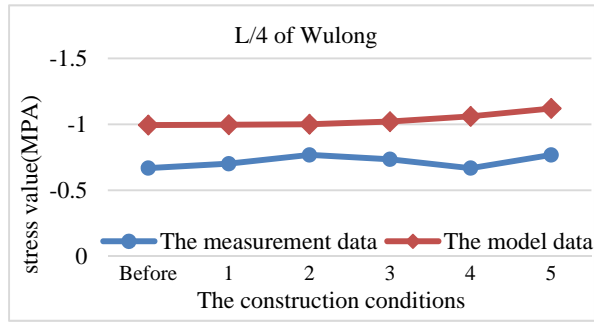


Fig.8. The change of stress on L/4 of Wulong

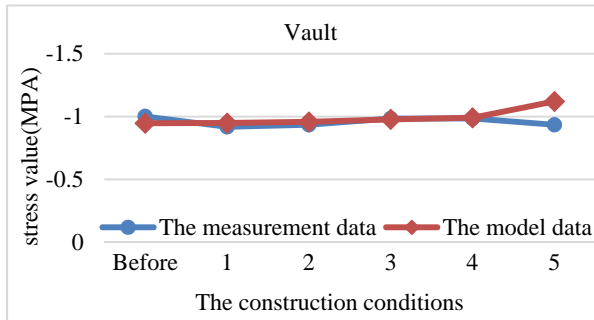


Fig.9. The change of stress on vault

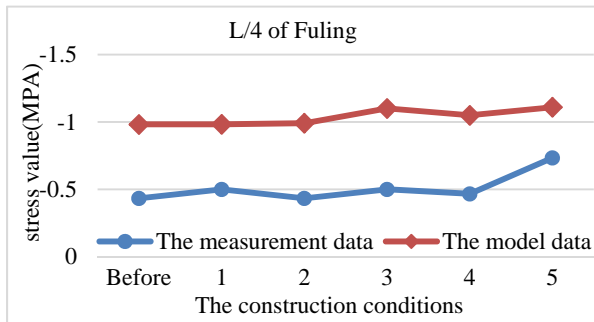


Fig.10. The change of stress on arch foot of Fuling

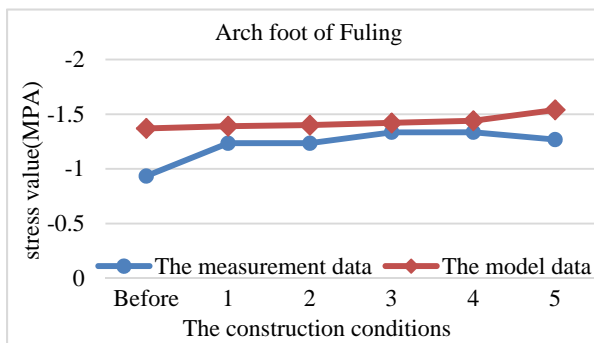


Fig.11. The change of stress on arch foot of Fuling

It is observed that the stress of arch foot, L/4 and vault have a tendency to gradually increase, however the variation is small. The stress on critical control sections for each construction stage are in state of

compression and no more tension stress. It shows that the stress of arch foot, L/4 and vault are reasonable. Accordingly, we can ensure that the stress measurement value on each section is less than the stress model value and the limit value. The main arch is within safe levels and stress which can meet the requirement of the specifications.

## 5. Conclusion

By deformation monitoring, stress measurement and the finite element model analysis for the construction stages of main arch reinforcement of DaXiHe No.3 Bridge, we can get the following main conclusions:

1. Vault is the most liable to deform in the process of reinforcement. It is followed by part L/4. The deformation of arch foot is particularly small. Because of the deformation being most easily detected in monitoring, the vault is the most important part of measurement on similar deformation monitoring in the future.

2. The stress on critical control sections on each construction stage are in state of compression. What is more, they have a tendency to gradually increase, however the variation is small. This shows that the adverse impact of C-S-C (concrete-stone-concrete) method on the original construction is very small and the integrity and bearing capacity of bridge are improved significantly. The good reinforcement effect of bridge will prolong the service life of bridge.

The bridge has been safe and stable during the construction process of the main arch. The deformation and stress monitoring of main arch provide valuable guidance and reference for the construction. Monitoring work shows the results are satisfying.

## References

- [1] Zhongfu Xiang. Bridge Engineering Control. Beijing: China Communications Press. 2011.
- [2] Yanran Yu, Wang bin. Technology research for JiuQuHe bridge reinforcement engineering's construction monitoring. Guangxi: Western China. 7, 2011, p.1-5 (in China).
- [3] Yun ling Li, Yun Meng. Application of Bonding Steel Plate to Reinforcement of Stone Arch Bridge. Journal Of Chongqing Jiaotong University (Natural Science) Vol. 26 Supplement, 2007.
- [4] Branson, D.E. Deformation of Concrete Structure, McGraw Hill Book Company, New York, 1977.
- [5] Larrard De, F., Acker, P. and Le Roy, R. Creep shrinkage and temperature effects, in High Strength-Performance Concrete (ed. S.H. Ahmad), Edward Arnold Publishers, New York, 1992.
- [6] Andrea Cavicchi, Luigi Gambarotta. Two-dimensional finite element upper bound limits analysis of masonry bridge, Computer and structures, 2006, 84:2316-2328.
- [7] Andrea Cavicchi, Luigi Gambarotta. Analysis of masonry bridges taking into account arch-fill interaction, Engineering Structures, 2005, 27:605-615.
- [8] Alex Rong. Structural Analysis of all Ancient Arch Bridge Using Modern Technology. Structures 2004. ASCE 2004:1-8.
- [9] Ying Luo, Huaneheng Tang. Study of China Masonry Arch Bridge. Beijing: China Communication Press, 1993.
- [10] Gaicedo J.M, Marulanda J, Thomson P, Dyke S J. Monitoring of bridges to detect changes in structural health. Proceedings of the American Control Conference; 2001; 1:453-458.
- [11] F.T.K.Au, J.J.Wang, G.D.Liu. Construction Control of Reinforced Concrete Arch Bridges, Journal of Bridge Engineering, 2003, 8(1), 39-45.





# The Summary of Clustering Methods on the Privacy Preserving

Shuang Gu<sup>1</sup>, Chi Ma<sup>2</sup>, Bao Li<sup>3</sup>, Meihui Wang<sup>4</sup>

<sup>1,2,3,4</sup>University of Science and Technology Liaoning School of Software, AnShan LiaoNing, 114004, china

<sup>2</sup>Corresponding author

**E-mail:** <sup>1</sup>m15904921460@163.com, <sup>2</sup>asmachi@126.com, <sup>3</sup>libao9303@163.com, <sup>4</sup>15904920910@163.com

## Abstract

Privacy preserving is an important direction in data mining. The purpose is to get mining results using data mining tools at the premise of disclosing private data. Researchers have proposed some algorithms for privacy preserving, these algorithms include both horizontally and vertically partitioned data, but only a few algorithms on privacy preserving clustering, and these algorithms with high complexity and low efficiency, mostly based on k-means, based on two parties or depend on a trusted third party. The security and reliability meet with the needs of users difficulty. This paper summarizes the features of privacy preserving clustering data mining algorithms by analyzing and comparing some current representative ones which include data modification, secure multiparty computation, anonymous in the light of data distribution. Furthermore according to the comparison, some evaluation standards are brought forward to develop new effective algorithms for future research, such as, the degree of privacy preserving, complexity of the algorithm, the efficiency of the algorithm, and analyze the influence of a variety of privacy preserving algorithms on clustering results.

**Keywords:** privacy preserving; clustering; data mining.

## 1. Introduction

Recently, Data mining technology has been rapid development and gained many achievements, however, produced the issues of information security and privacy protection at the same time. One of the recent research focus in the field of data mining is how to dig out the useful information while maintaining privacy. The clustering is an important research in the field of data mining. There are many kinds of clustering methods[1], such as partition-based methods, density-based methods, grid-based methods, model-based methods and so on. This article will describe the problem of the privacy protection in the process of clustering, and discusses clustering techniques based on privacy protection. There are two requirements clustering mining based on privacy protection: can't share individual privacy data while clustering; privacy can be not deduced from the results of mining. Today, many privacy protection technologies are proposed in different data mining models. the main methods including data conversion, secure multi-party protocol and k-anonymization methods etc. The idea of clustering-based privacy protection of data conversion is to make real sensitive data unknown through matrix to transformation data, and then conduct clustering analysis. Clustering based on secure multi-party protocols, mainly by constructing secure multi-party protocol; make a group of participants that will eventually learn the global clustering information in the case of only to have their own private information. Secure Multiparty Computation is generally used for a distributed database. The aim of based on k-anonymization is to

resolve the problem of privacy leaks due to link attack.

## 2. Privacy Protection Technology Based on Data transformation

Data transformation technique is a primary method of data perturbation method, which is a common method to solve privacy protection in the data mining. The main idea of data perturbation technique is to protect the effectiveness of data mining and statistics, meanwhile, to make the real data value of individual or department not be disclosed by converting the data. Because the converted data can't reflect the real data value of individual or department, so even if the data item is associated with an individual, the individual's privacy will not be violated. One of the main methods of perturbation technologies is data transformation [2], which hided the real data value by converting data records, but ensured a reliable statistical result at the same time.

Stanley R.M. Oliveira described in detail several common data transformation methods in the literature[2], including Translation Data Transformation process(TDP) 、 Scaling Data Transformation Process(SDP)、 Rotating Data Transformation Process(RDP)、 Hybrid Data Transformation Process (HDP) ,here is not introduce more.

### 2.1 Privacy protection method based on isometric transformation data

Isometric transformation is that if  $T : R_n \rightarrow R'_n$  is a transformation of an n-dimensional space,for any two points  $P$  and  $q$  in  $R_n$ ,meet  $|T(p) - T(q)| = |p - q|$ ,so  $T$  is called an isometric transformation of

$R_n$ .Privacy protection degree is represented by  $\rho = \text{var}(X - X')$ ,wherein  $X$  represents a property value before perturbation, and  $X'$  represents a property value after perturbation, and  $\text{var}(X) = \text{var}(x_1, x_2, \dots, x_n) = \frac{1}{n} \times \sum_{i=1}^n (x_i - \bar{x})^2$ ,wherein  $\bar{x}$  is the average value of  $x_1, x_2, \dots, x_n$ .

RBT algorithm[5] is an improved rotation algorithm on the basis of simple rotation. RBT algorithm to avoid misclassification of data points just by rotating property vector pairs. Secondly, standardize the data before converting the data. The purpose of standardization is to keep the correlation between the data points, simultaneously, to better protect the original property value, finally, get the correct clustering results. The main process shown in Figure 1.

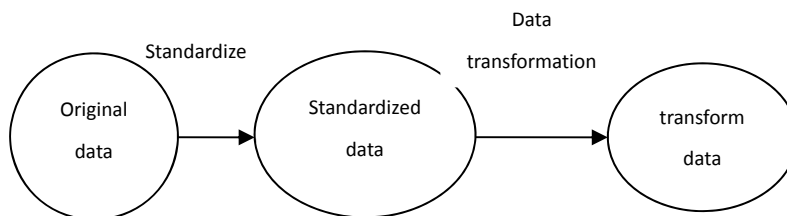


Figure 1 RBT algorithmic process

The first step is data standardization. There are generally two standardization methods: MIN-MAX

standardization and Z-SCORE standardization.

The second step is data transformation. The step of data transformation is that assumed that standardized data matrix is  $D$ , privacy protection degrees are separately  $\rho_1, \rho_2$ . The step of the transformation is that firstly, select the property vector pairs. Select  $k$  pairs of property vector  $A_i$  and  $A_j$ ,  $i \neq j$  in  $D$ . If the number of property is even, then  $k = n/2$ , otherwise  $k = (n+1)/2$ . Note that the selection of property vector pairs is not continuous, The way to select safely is that arbitrarily select property vector pairs, if  $n$  is odd, then last selected property and any converted property has been combined again, after transform property vector pairs. ① Isometric transform property vector pairs, which makes  $V(A'_i, A'_j) = R \times V(A_i, A_j)$ , wherein  $V(A_i, A_j)$  represents the corresponding values of  $A_i$  and  $A_j$ . ② Solve the range of  $\theta$  that is required by privacy protection degrees of  $\rho_1$  and  $\rho_2$ .  $\theta$  must meet the condition of  $\text{var}(A_i - A'_i) \geq \rho_1$  and  $\text{var}(A_j - A'_j) \geq \rho_2$ , wherein  $\rho_1 > 0, \rho_2 > 0$ . ③ Randomly select  $\theta$  that satisfies some conditions, bringing it into the transformation formula of ①, calculate converted property vector pairs of  $A'_i$  and  $A'_j, i \neq j$ .

Geometric data transform method [3] and RBT algorithm for privacy protection is simple and efficient, these methods are intended only for data processing before clustering, therefore, data perturbation method is independent of various clustering methods. In other words, such methods are generally applicable to any clustering algorithm, and have a more reliable mathematical foundation. Simple translation, scaling and rotation will change the correlation between data points, RBT algorithm has been improved for this problem, and use privacy protection degree to determine selected range of converting the angle, and to ensure that it has good effects of privacy protection in most cases.

Data transform algorithm[4] based on isometric transformation maintains a constant distance between two points in the process of perturbation, it could very well perturb the data, protect privacy, while allowing clustering results are not affected. When RBT transforms any paired property vector pairs, randomly selects one isometric transformation to transform, in the process of transformation, the relative privacy protection degree according to be required determines selected range of converted angle  $\theta$ , ultimately, select randomly converted angle in the range meet the requirements.

## 2.2 Privacy protection clustering based on orthogonal transformation

It proposed conversion method of orthogonal transformation (OBT) on the basis of RBT, and make use of proved theorem to establish matrix library in advance, make not to require a lot of computation time when transforming. Certainly, in which it is not always necessary for all  $n$  properties of the original data to transform, take into efficiency account, the most common situation is to transform for several joint properties step by step. In fact, do a orthogonal transformation for a joint property is equivalent to all the properties to do a joint orthogonal transformation, and orthogonal transformation closed on multiplication, which ensures a series of results of orthogonal transformation of joint properties is ultimately an orthogonal transformation for the original data.

OBT does mainly orthogonal transformation on any paired pairwise independent property vectors, for

every property vectors, randomly selected an orthogonal matrix that meets the requirements to orthogonal transformation from matrix library, and then outputs the transformed data. Firstly algorithms assume that the data matrix is personal numerical data that must be converted to protect before only included in clustering, and data has been standardized by z-score method; of course, property vectors must also be pairwise independent and need to convert enough data. In the transformation, there are two key steps:

Establish a matrix library, this part may be done before transforming, and can build any dimension orthogonal matrix library to meet the minimum requirements of the privacy protection, but in the general case, it is enough to build only two and three dimensional matrix library.

Select and transform property vector pairs. Property vector transformed is pairwise independent, in order to simple calculation, it commonly used every two property vectors make a pair, each of the two properties of vectors  $o_i, o_j, i \neq j$  are randomly divided into a pair; if the number of property vector is odd, finally the remaining three are paired, and randomly select the orthogonal matrix are exchanged from the matrix library.

According to Johnson-Lindenstrauss's theorem [7], the distance between the data points of high-dimensional feature space to low-dimensional feature space remains basically unchanged, which proposed privacy protection clustering method based on random orthogonal matrix. The experimental results show that this method is simple, but which played a role in protecting privacy under the circumstance of doing not affect the clustering results.

### 3. Clustering algorithm based on secure multiparty protocols

Yao first proposed problem of secure both parties computation in 1986, next which evolved problem of secure multiparty computation. It first combines systematically secure multiparty computation (SMC) problem and privacy protection data mining [8]. The definition of SMC problem is a group of participants calculated mistrust each other; they want to agree on a secure function, and the input function is provided by the participants, and function should ensure that each participant can still get the correct results even if in the case of dishonest participants, and can only get the results of the pre-set function, the input of each participant relative to other participants is invisible. When there is dependable other, SMC problem does not exist, but it is difficult to find dependable other party in reality, or does not exist at all. SMC problem is to discuss based on the absence of a dependable third party, and more for protecting sensitive data in a distributed environment.

Security protocol to protect data privacy, first obtains  $k$  initial cluster centers using hierarchical clustering algorithm, and then uses  $k$ -means clustering algorithm to obtain accurate  $k$  clusters. In order to reduce IO operations, reduce traffic, reduce the workload on secure multiparty computation, improve computational efficiency, to build identification information (sites, object identity) of linear form storing  $n$  objects in SP party, the object here is identify through data party encrypted, and the linear form of permanent memory. Meanwhile, in order to get the distance between all points in the data matrix, it needs to construct the dissimilarity matrix. Dissimilarity matrix is a cluster-cluster structure, dissimilarity matrix  $d$  of  $n \times n$  stores distance between  $n$  clusters or dissimilarity,  $d_{ij}$  represents the distance between the cluster and the cluster of the first  $i$ - $j$ , in  $d_{ii} = 0, d_{ij} = d_{ji}$ . Therefore, there are only elements below the diagonal stored in the matrix. Each data party to build its local dissimilarity matrix and send it to SP, SP

collects sent local dissimilarity matrix from parties and the distance between the point-to-point from different parties, and get the global dissimilarity matrix. And using of clustering feature tree to describe the cluster structure, and SMC protocols use cluster analysis to solve the problem of privacy protection methods, it not only good for privacy, but also to ensure the accuracy of mining results. however, existing solutions are only for the problem of cluster analysis privacy protection using Euclidean distance to measure the distance between data, and for others, such as density-based clustering, connection-based clustering, the problem of cluster analysis privacy protection cannot put a good solution to the need for further analysis and research.

#### **4. The clustering of privacy protection based on anonymous**

Recently, many studies of privacy protection have focused on the protection of the individual identification information in the shared data set, privacy protection model[9] about this aspect are mainly: k-mapping, k-uncertain and k-anonymization.

K-mapping aims to make the target data in each record must be at least corresponding to the entities in k external data source. This prevents the user to connect an external data table to determine the identity of the owner of the data record. However, the external data source is not the only in many cases, therefore, specific programs of privacy protection is difficult only determined. the issue by the external data source brought about the uncertainty is eliminated by The k-anonymity model, further requires that tuples of target data set corresponding to the individual is difficult to distinguish with other tuples corresponding to the individual. When the owner of data publishes data set, it usually remove the property field(often declare the primary key or “unique” ) able to directly identify the individual, such as name, identify card number. However, some seemingly less important properties of non “unique” combined, often only able to determine the identify of the individual. In the data set[9] treated by k-anonymity algorithm, any tuple are able to find at least  $k \geq 2$  other tuples, and makes these tuples on all the “quasi-identifier” property has the same property value. Thus, the user can not distinguish from the individual is represented by k tuples. As k-uncertainty model, it does not only require more than the property of k tuples on the composition of the “quasi-identifier” have full equal value, but also requires that can not distinguish between different tuple “quasi-identifier” , it is a generalized form of k-anonymity model, but informed the statistical results on “quasi-identifier” on the rear, and k-uncertainty model may disclose specific property values on “quasi-identifier” .

The process of k-anonymity is mainly achieved by generalizing the property value. Due to the theory demonstrates that using generalization operation to achieve k-anonymity is the NP-Hard problem, therefore, using different strategies to optimize the process of generalization of this data is anonymized research’s focus. This includes the global generalization according to properties and partial generalization according to tuple. Document[9] provides tools that could balance the characteristics of global generalization and partial generalization. Meanwhile, the method of constructing the overall classification tree on the data collection of k-anonymity more than satisfied, as well as data collection on multiple related data sheets or continuous increase in the implementation of anonymity also recently been proposed. Except through generalizing and suppressing operations to deal with quasi-identifier property, the document[10] also used a clustering algorithm to anonymize data collection.

#### **5. Assessment of algorithm**

The degree of privacy protection: in order to compare the level of different transformation for privacy

protection methods to assess data security by group database to assess the degree of privacy protection. the degree of privacy protection  $\rho = \text{var}(X - X')$ , wherein  $X$  represents a property value before perturbation, and  $X'$  represents a property value after perturbation, further

$$\text{var}(X) = \text{var}(x_1, x_2, \dots, x_n) = \frac{1}{n} \times \sum_{i=1}^n (x_i - \bar{x})^2, \text{ wherein } \bar{x} \text{ is the average value of } x_1, x_2, \dots, x_n. \text{ These}$$

assessments are worth out based on the number of property value after perturbation close to the original. In addition, in privacy protection, you need to assess how likely the transformed data may be estimated, may be referred to the uncertainty of privacy. There is no uniform standard to the uncertainty in the quantitative determination of this indicator of privacy. The ultimate goal of privacy is to prevent some unauthorized operation to destroy the privacy of information or disclosure certain sensitive information, therefore, we should guard attackers and against data theft who use a variety of data mining algorithms to discover and mining their own privacy data information, greater chance of reducing the hidden information is used by some way directly accessed and increase the ability of resisting malicious party to cheat.

The performance of algorithm: the main consideration is the cost of time and costs of transportation between both parties. That is contrast that the complexity of need of the algorithm hides a particular collection of sensitive information, the cost of calculation higher, indicating that the lower the performance of the technology; the complexity of the transmission higher, the lower performance. Usefulness of the data: the final stage of the process of privacy protection data mining, that need to consider the usefulness of the data, this is a very important indicator, and privacy protection of the usefulness of the data includes two aspects: protecting privacy information and ensure of the greatest degree the usefulness of the data, and privacy protection is the hardware requirements that must be met, and the usefulness of the data required to achieve optimal. To hide sensitive data, such as the use of perturbation technology on the original data, will result in loss of information accuracy, and precision loss depends on techniques of data mining on the use of data, such as clustering, accuracy loss can be achieved by comparing the results before and after clustering privacy.

Expansibility: in addition to the above evaluation index of the effectiveness, based on the evaluation index of the efficiency has also been extended. considered on the basis of the cost of computation plus expansibility index, including the ability to handle high-dimensional data, and the capabilities to process different data types, and full account of the implementation of this algorithm on the expertise requirements (mainly refers to the parameters' identification and selection).

## 6. Conclusion

This paper does a certain presentation and analysis for the current typical algorithm, and comprehensively proposed evaluation criteria of that the algorithm of privacy protection data is good or bad. These algorithms are not very different in practical aspects of data, and the data can be well protected in the aspect of privacy protection degree, so that your personal information or sensitive information will not be disclosed, while clustering results were not affected. However, due to clustering problem is not as mature as the association rules, and also not as widely used as association rules, together with the privacy issue is just being people pay attention to it in recent years, so the privacy of clustering algorithms are still many shortcomings and deficiencies. For example, most of the existing algorithms for privacy preserving

clustering is processed for numeric data, and treatment for other types of data is quite rare, and there is a certain complementarity between some algorithms, how to combine the different algorithms in order to improve the performance and applicability of the algorithm to improve the degree of privacy protection, will be an important direction we need to study in the future.

### Reference

- [1] Jiawan Han, Micheline Kamber Write, Ming Fan, Xiaofeng Meng Translate. Mechanical Industry Press.
- [2] Stanley R M Oliveira , Osmar R Zaiane. Privacy Preserving Clustering By Data Transformation[C],PPProc. of the 18th Brazilian Symposium on Databases , Manaus , Brazil , 2003 :304 - 318.
- [3] Weiwei Huang , Wenyang Bai. Geometry Data Conversion through Privacy Preserving Clustering Mining[J].Application Research of Computers,2006 ,23 (6) :180 – 181.
- [4] Stanley R M Oliveira , Osmar R Zaiane. Achieving Privacy Preservation When Sharing Data for Clustering[C] PPProc. of the International Workshop on Secure Data Management in a Connected World , 2004 :67 - 82.
- [5] S R M Oliveira, O R Zaiane. Achieving Privacy Preservation When Sharing Data for Clustering[C]. Toronto: Proc. of the International Workshop on Secure Data Management in a Connected World ( SDM'04) in Conjunction with VLDB, 2004. 67282.
- [6] Guorong Zhang, Jian Yin. Privacy Preserving in Clustering through Isometric Transformation.Application Research of Computers, 2006,7
- [7] Dr. Meera Sitharam. Lecture:Johnson-Lindenstrauss Lemma and Embedding the diamond graph in Lp. Geometric Constraints CIS 6930,2006.
- [8] Lin Yang, Xiaping Zhang, Zhiguo Bai, Hui Xu, Lin Lin.Research of Clustering Analysis Privacy Protection based on SMC protocol.Computer Engineering and Design.2008.11.Vol 29





# Experimental Data Publishing Based on Browser/Server for Neutral Beam Injection in EAST

Sheng Bai<sup>1</sup> Yang Liu<sup>2</sup>

<sup>1,2</sup> School of Northeast Petroleum University, Heilongjiang 163318, China

<sup>1</sup>Corresponding author

**E-mail:** <sup>1</sup> [iambaisheng@hotmail.com](mailto:iambaisheng@hotmail.com)

## Abstract

In the experiment of Neutral Beam Injection (NBI), Experimental Data Publishing Software (EDPS) is developed to get experimental data monitored remotely. Adopting B/S module, EDPS publishes information, such as experimental configurations and results on the Internet dynamically. The design and implementation of how EDPS uses the present information source in NBI Control System (NBICS), the procedure EDPS handles the requests from clients and displays the information on web pages are introduced in this paper.

**Keywords:** NBI, B/S, data, experimental results, publishing, AJAX, JFreeChart..

## 1. Introduction

NBI system is employed on Experimental Advanced Superconducting Tokamak (EAST) for plasma heating and plasma current driving to support the steady-state operation and physical research [1]. NBICS is a subsystem which takes charge of monitoring the experimental operation process and interlock protection. Besides, it implements data collection processing and network communication [2]. During the experiment, NBICS collects experimental configuration, current value and voltage value of magnet power supply, gas valve, arc power supply, etc. This information makes great contribution to experimental result analysis.

EDPS acquires experimental data and publishes them on the Internet. With the implementation of EDPS, users who cannot get access to the Local Area Network (LAN) of NBI system can get an approach to experimental data acquisition.

## 2. Requirement and Analysis of EDPS

NBICS consists of four levels: remote control level, main control level, field control level and video monitoring level [3]. In each discharge, Main Control Console (MCC) in remote control level sends configuration to Main Control Server (MCS) which is located in main control level. Then MCS transmits the command to subsystems and acquires the results collected in field control level. In this process, MCS saves all configurations and results. For the sake of analyzing the data, this information needs to be published beyond the LAN. Take security into consideration, MCS needs to be isolated from Internet in case that the data are modified illegally. So a platform connected with main control net and Internet is established. EDPS is software running on this platform, collecting experimental data and publishing them on the Internet. EDPS is implemented with the following specific functions:

- a. During the experiment, EDPS displays the current configurations of the experiment, including shot number, voltage, and amplitude and pulse width of each sub-system.
- b. EDPS displays experimental results collected by different channels in the form of waveform dynamically.
- c. EDPS offers inquiry service for historical data, such as experimental configurations, spectrum results, etc.

**3. Implementation**

EDPS adopts B/S model. Clients can access data on the server by using a browser. This model decreases the burden of clients and developers. Besides, it provides an easier way to update software. The architecture of EDPS is shown in Fig. 1 (parts in dotted box). Data acquisition module takes charge of the communication with MCS to acquire experimental data. Request processing module processes requests from clients and transmits data between server and web page display module. Web page display module displays experimental data in appropriate forms on web pages.

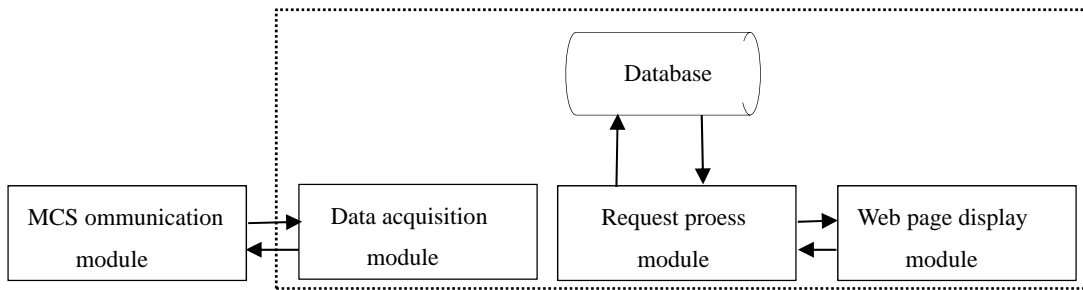


Fig.1 Architecture of EDPS(parts in dotted box)

**4. Design of Data Acquisition Module**

In this module, programs standard TCP/IP protocol structure is defined as it is are developed in C/C++ language, with a C/S program model based on and multi-threading technology. The NBI TCP communication data structure is defined as it is shown in Fig.2. The numbers at the top of figure express the size of bytes in different fields[4]. In every discharge, MCS sends information under this structure then EDPS analyzes the information and an interface for request processing module. Saves the data into MySQL database thus provide.

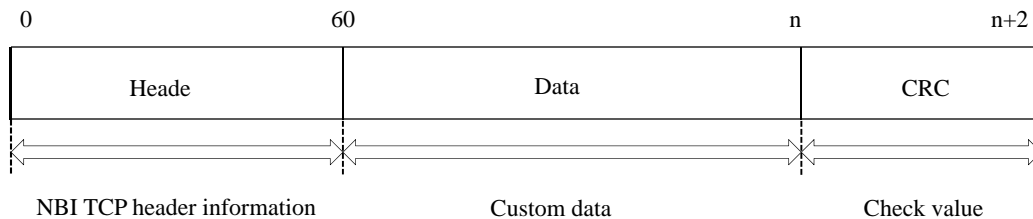
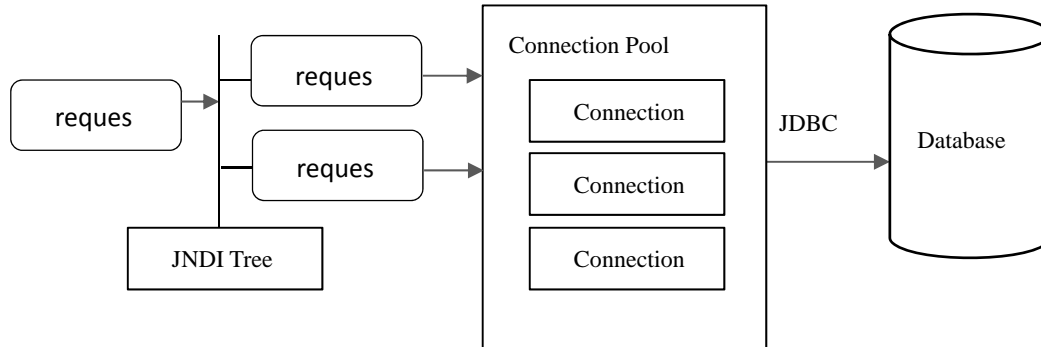


Fig.2 Definition of the NBI TCP communication data structure

**5. Design of Request Processing Module**

In this module, Java Web techniques, especially servlet, Asynchronous JavaScript and XML (AJAX) are applied to process requests from clients. Taking advantages of specific class, servlet based on Java

checks whether the requests is legal, then servlet invokes specific Java Bean to handle the requests and transmits responses to Web page display module or AJAX programs. Java Bean mainly handles the database by taking advantage of the application of connection pool. The work procedure of Java Bean is shown in Fig. 3.



**Fig.3** Work procedure of Java Bean

AJAX is adopted to implement partial update of web pages in order to avoid the waste of bandwidth [5]. The programs are developed by JavaScript which are embedded into Hypertext Markup Language (HTML) or Java Server Page (JSP). Since experimental data change dynamically, AJAX programs send requests to servlet in every period to get the new information from database. In this way, web pages are refreshed dynamically to show the changes. The application of AJAX frameworks optimizes this module.

**6. Design of Web Page Display Module**

Experimental data are published in the form of table and waveform. This module is developed mainly relying on JSP and HTML. Some configurations are shown in the form of tables which can be directly printed on web pages, while other data, such as the amplitude and pulse wide of power supply, results collected from different channels are better to be displayed in the form of waveform.

Waveform is generated by JFreeChart, which is a library developed by Java. This library supports for many output types, including Swing components, image files (including PNG and JPEG), and vector graphics file formats (including PDF, EPS and SVG) [6]. In this module, waveform is imported by image files. Apply data by using the Class 'chartUtilities' and use themethod 'writeChartAsJPEG' to output image in format of JPEG. Using the method 'writeRenderingInfo' can generate MAP data. MAP data enables clients to read the accurate value of each point of the waveform by keeping the mouse pointer staying. The work flow of generating waveform by JFreeChart is shown in Fig. 4.

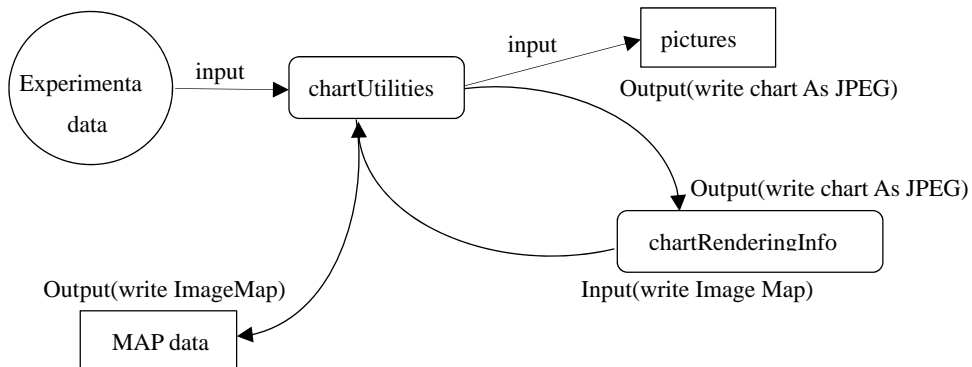


**Fig.4** Work flow of generating a waveform by JFreeChart

## 7. Conclusion

The design and implementation of each sub module of EDPS are described in this paper. EDPS meets the requirements of publishing configuration and experimental results dynamically and providing service for inquiry. By adopting B/S, EDPS provides a method to analyze experimental data for those people on the Internet network.

## References

- [1] Hu Chundong, Xie Yahong, 2011, Plasma Science and Technology, 14:75
- [2] Sheng Peng, Hu Chundong, Song Shihua, et al. 2013, Plasma Science and Technology, 15:6
- [3] Sheng Peng, Hu Chundong, Song Shihua, et al. 2010, Asia Pacific conference on plasma science and technology, Jeju Island, Korea, pp. 4-8
- [4] Wu Deyun, Hu Chundong, Sheng Peng, et al. 2013, J Fusion Energy, 1:5
- [5] Huang X T, Yang B Z, et al. 2010, Computer Engineering and Design, 31:2629
- [6] D. Gilbert, 2002, "The jfreechart class library," Developer Guide. Object Refinery